https://doi.org/10.5194/egusphere-2025-5520
Preprint. Discussion started: 18 December 2025

Three decades of snow water equivalent dynamics in the Po River Basin, Italy: Trends and Implications

John Mohd Wani[1], Kelly E. Gleason[2], Matteo Dall'Amico[3], Federico Di Paolo[3], Stefano Tasin[3], Gaia Roati[1,4], Marco Brian[4], Francesco Tornatore[4], and Riccardo Rigon[1,5]

[1]C3A - Center Agriculture Food Environment, University of Trento, San Michele all'Adige, Trento, Italy
[2]Department of Environmental Science and Management, Portland State University, Portland, Oregon, USA
[3]Waterjade Srl, Pergine Valsugana (TN), Italy
[4]Po River Basin District Authority, Parma, Italy
[5]Department of Civil, Environmental and Mechanical Engineering, University of Trento, Trento, Italy

Correspondence: John Mohd Wani (johnmohd.wani@unitn.it) and Riccardo Rigon (riccardo.rigon@unitn.it)

Abstract.

Seasonal snowpack is a key component of the mountain cryosphere, acting as a vital natural reservoir that regulates runoff downstream in snowfed basins. In mid- and low-elevation mountain regions such as the European Alps, snow processes, such as accumulation and ablation, are highly sensitive to climate change, having direct implications for hydrological forecasting and water availability. In this study, we present the analysis of a 30-year (1991–2021) long dataset of snow water equivalent (SWE) in the Po River District, Italy, which includes parts of the Alps and Apennines. The data is available at a 500×500 m^2 spatial resolution and at a daily temporal scale (Dall'Amico et al., 2025). This data was generated using the "J-Snow" modeling framework, which integrates the physically based GEOtop model with in situ snow height observations and earth observation snow cover products such as MODIS. Our results show that the long-term (30 year) basin-wide mean annual SWE volume equals 3.34 Gm^3. The elevation-wise statistical analysis of key snow volume and duration metrics shows that the most pronounced snow water equivalent losses occur below 2000 m a.s.l. Below this threshold, both snow volume metrics and duration metrics show a significant decrease, indicating decrease in snow water storage and earlier melt. Above this elevation, the snow volume metrics show increasing trend while as the duration metrics continue to show a shortened (decreasing trend) snow season except at the highest elevations (>2500 m). The findings of this study highlight the changes to the mountain seasonal snow storage and the timing of snow dissappearance across the Italian Alps. This combined effect highlights a fundamental shift in the hydrological regime of the Po River Basin, with significant implications for water availability and management under ongoing climate change.

1 Introduction

Global warming has significant effects on the cryosphere (Hock et al., 2019), with mountain regions, particularly the European Alps, experiencing more warming (twice) (cf. (Kotlarski et al., 2022)) relative to the global average (Copernicus, 2025; Kotlarski et al., 2022). According to the Sixth Assessment Report (AR6) of the Intergovernmental Panel on Climate Change

https://doi.org/10.5194/egusphere-2025-5520
Preprint. Discussion started: 18 December 2025

(IPCC), global surface temperatures increased by 0.99 [0.84–1.10]°C between 2001 and 2020 compared to 1850–1900 levels (IPCC, 2023). The rising surface temperatures in mid-latitude mountain ranges like the European Alps is projected to lead to a change in the precipitation phase from snow to rain, resulting in earlier snow-melt runoff (Dozier, 2011; Hock et al., 2019). In the European Alps, this warming has already led to a reduction in snow cover (Notarnicola, 2022) and snow depth (Matiu et al., 2021; Bozzoli et al., 2024). The warming-induced changes in snow is having critical implications for downstream water availability (Avanzi et al., 2024; Montanari et al., 2023; Zampieri et al., 2015), ecosystem functioning (Edwards et al., 2007; Colombo et al., 2023) and socioeconomic impacts (Abegg et al., 2007). During the last century, spring discharge in the largest Alpine River basins (Rhine, Danube, Rhone, and Po) has consistently shifted two to three weeks earlier, partly due to changes in snowmelt timing (Zampieri et al., 2015).

Seasonal snowpack is an important part of the European Alpine climate system because it acts as a reservoir, storing water and subsequently releasing it, thus playing a vital role in the hydrological cycle (Matiu et al., 2021) and, in the Italian Alps, SWE contributes about 50% of the total river runoff (Avanzi et al., 2023). In addition, it also plays an important role in the energy budget due to its high albedo and low thermal conductivity (Edwards et al., 2007). From an economic point of view, the amount and duration of snow is very important for tourism and hydropower generation (Marty, 2008). For example, in the Alps, many villages and towns are highly dependent on winter tourism for their livelihood (Abegg et al., 2007).

The snow cover area (SCA) has been the basis for snow monitoring efforts (Brown, 2000; Notarnicola, 2022, 2020), however, the SCA does not provide direct information on the water content stored in the snowpack (Brown, 2000; Sturm et al., 2010; Huning and AghaKouchak, 2020). To understand the changes in water availability associated with the volume and timing of snow storage we must focus on the snow water equivalent (SWE) (Sturm et al., 2010) since it provides a fundamental measure of the volume of water contained within the snow (Huning and AghaKouchak, 2020; Avanzi et al., 2024). SWE is defined as the equivalent amount of water that would result after melting the entire snowpack (Egli et al., 2009; Huning and AghaKouchak, 2020). Traditionally, SWE is measured on a point-scale using snow courses and snow pillows (Serreze et al., 2001), and these represent a small footprint of the area of actual ground conditions (Dozier, 2011; Molotch and Bales, 2006), providing limited information on spatial variability, especially in data-scarce high-elevation mountain regions (Ma et al., 2023; Dozier, 2011). Furthermore, the combination of mountain topography and weather systems amplify this limitation, highlighting the need for a temporally continuous and spatial distributed SWE dataset, such as the one used in this study (Dall'Amico et al., 2025).

At a spatially distributed scale, SWE data are generally reconstructed from remote sensing techniques (Premier et al., 2023; Oveisgharan et al., 2024; Tsang et al., 2022; Schilling et al., 2024), data assimilation of remote sensing, reanalysis and modeling (Margulis et al., 2019, 2015; Avanzi et al., 2023; Dall'Amico et al., 2025). The latest active remote sensing techniques like Synthetic Aperture Radar (SAR) (Tsang et al., 2022), Interferometric SAR (InSAR) (Premier et al., 2023; Bonnell et al., 2024) and lidar-based (Kwon et al., 2021) allow for reconstruction of finer-scale SWE. However, estimation of SWE at spatial scale from remote sensing is still a challenge due to accuracy, spatial, and temporal resolution due to topography, vegetation, etc. (Oveisgharan et al., 2024; Tsang et al., 2022; Bonnell et al., 2024). Even if the SWE can be reconstructed based on the integration of a simulated melt flux over the time period of remotely sensed observed snow cover, this method generates data only on the peak SWE value and introduces errors when snowfall occurs during the melt season (Durand et al., 2008;

https://doi.org/10.5194/egusphere-2025-5520
Preprint. Discussion started: 18 December 2025

Molotch, 2009). Therefore, the dataset used in this study was generated using a hybrid modeling approach, which integrates the physically based GEOtop 2.0 model (Endrizzi et al., 2014) with a multi-source data assimilation framework that incorporates both in situ and EO data which allows to generate a continuous spatio-temporal SWE dataset (Dall'Amico et al., 2025; Avanzi et al., 2023).

Snow droughts is defined as the deficit in the SWE especially in winter (Huning and AghaKouchak, 2020; Colombo et al., 2023). Their frequency and duration can have serious implications in snowfed basins (Huning and AghaKouchak, 2020; Colombo et al., 2023) and subsequently result in streamflow drought in the melting season (Chartier-Rescan et al., 2025). Globally, in the recent past, snow drought has become more frequent and worrying phenomenon (Huning and AghaKouchak, 2020). As an example, In summer 2022, Northern Italy faced an exceptional snow drought (Koehler et al., 2022; Avanzi et al., 2024; Colombo et al., 2023; Chartier-Rescan et al., 2025) severely impacting the Po River Basin (Avanzi et al., 2024; Chartier-Rescan et al., 2025; Montanari et al., 2023) and the recorded SWE was the lowest in the last 100 years (Colombo et al., 2023).

This raises the critical question of how SWE patterns have changed over the long term in the Po River Basin. The study area's location in a climate transition zone between the Mediterranean and Northern European regions makes this investigation particularly relevant (LIFE CLIMAX PO Project, 2023). This transitional position renders the region especially vulnerable to climate change impacts, highlighting the urgent need for evidence-based adaptation and mitigation strategies (LIFE CLIMAX PO Project, 2023). Therefore, the high-resolution SWE record (Dall'Amico et al., 2025) represents an invaluable resource for assessing how SWE has responsed to climate change in one of Europe's second most climate-sensitive River Basins (Carrer et al., 2023). This study presents a comprehensive analysis of long-term SWE trends in the Po River Basin, Italy, using a 30-year dataset spanning 1991–2021 (Dall'Amico et al., 2025). We address three key research questions: What are the long-term trends of SWE in the Po River Basin over the 1991–2021 period? How do long-term SWE trends vary across the elevational gradient in the Po River Basin? What climate drivers influence these long-term trends in SWE in the Po River Basin?

2 Study area and data

2.1 Study area

The Po River Basin is the largest in Italy (Fig. 1), with a drainage area of approximately 87,000 km^2. The Po River Basin is the main basin contained in the Po River District (Fig. 1, red and dashed), an overregional entity born by decree in 2015 as the union of the Po River Basin with some smaller basins, like the ones of Conca and Reno, that flows into the Adriatic Sea. This territory spans eight Italian regions: Aosta Valley, Liguria, Emilia-Romagna, Piedmont, Tuscany, Lombardy, Marche, Veneto and the Autonomous Province of Trento and some parts of Switzerland and France (LIFE CLIMAX PO Project, 2023). The Po River Basin is home to about 20 million people roughly one-third of Italy's total population (LIFE CLIMAX PO Project, 2023). This region includes more than 3 million hectares of agricultural land, contributing to more than 40% of the country's GDP, and producing roughly 55% of Italy's hydropower (LIFE CLIMAX PO Project, 2023).

https://doi.org/10.5194/egusphere-2025-5520
Preprint. Discussion started: 18 December 2025

The river has a total length of 652 km and originates from Monviso in the Cottian Alps in Piedmont and drains into the Adriatic Sea north of Ravenna, Italy. Along its path, the river receives water from 141 tributaries (of which 38 are the main ones) both from the Alps and the Apennines. These two mountain ranges create distinct hydrological regimes: (a) Alpine tributaries are characterized by snow and glacier melting with peak discharge in early summer, while (b) Apennine rivers are dominantly fed by rainfall and for this reason often experience significant low-flow or dry conditions during the same period (ADBPO, 2006).

The climate of the Po River District is strongly governed by its complex orography. In the North, the Alpine system acts as a barrier against Northern cold air masses, while the Apennine range prevents the moderating effects of the sea on the Po Valley. Together, these mountain systems trap humid westerly winds and alter the trajectory of Atlantic cyclones, shaping the spatial and seasonal distribution of temperature and precipitation in the Basin (ADBPO, 2006). The mean annual precipitation is approximately 1000-1200 mm (De Lannoy et al., 2024; ADBPO, 2006). The Po River Basin has a complex and variable precipitation pattern, which is divided into five types: (a) continental type, with summer maxima and winter minima, prevails mostly in the high Alpine valleys, (b) sub-littoral Alpine, and (c) sub-littoral western types are marked by two rainfall peaks, with the former showing a slight spring prevalence and the latter a more pronounced spring maximum, (d) sub-littoral Padano regime, with equivalent bimodal peaks, covers the central plain, while the (d) sub-littoral Apennine type, distinguished by a dominant autumn maximum, characterizes the southern portion of the basin (ADBPO, 2006). The mean annual temperature typically ranges from 5° C in the Alpine areas to 15° C in the plains and foothills of the Apennines (ADBPO, 2006).

This study focuses specifically on the mountainous part of the Po River District (Fig. 1, black dashed boundary), an area of approximately 51,000 km^2 that includes parts of the Alps and Apennines. It is characterized by a significant elevation gradient, ranging from the plains (0 m a.s.l.) to over 4,000 m a.s.l.

2.2 Data

In this study, we analyze a comprehensive 30-year long-term SWE dataset in the Po River Basin (Dall'Amico et al., 2025). The dataset is available on a daily time scale with a spatial resolution of 500 m^2 that partially covers the mountain ranges of the Alps and Apennines. This dataset is unique due to its long (1991-2021) temporal coverage and fine (500x500 m^2) spatial resolution, making it one of the most complete spatial SWE time series currently available for the study domain. Its homogeneity and consistency across a large spatial domain make it well-suited for applications such as water resource monitoring, snow-water storage assessment, snow drought analysis, snow dynamics, and snow climatology. Another gridded SWE dataset available for the Italy is the IT-SNOW (Avanzi et al., 2023) available at a resolution of 500 m from 2010 to 2021 with possible future updates annually.

In contrast to snow depth measurements, which do not directly represent the amount of water available from the snowpack, the SWE data enables quantification of the volume of water, an essential variable for water resource management and runoff forecasting (Huning and AghaKouchak, 2020). Furthermore, this dataset can serve as a reference for calibrating and validating temperature-index snow models (Formetta et al., 2014; J. G. Arnold et al., 2012), thus evaluating their reliability in both research and operational hydrological applications.

https://doi.org/10.5194/egusphere-2025-5520
Preprint. Discussion started: 18 December 2025

This dataset was generated using the hybrid modeling approach "J-snow" (Dall'Amico et al., 2018), which integrates the physically based GEOtop 2.0 model (Endrizzi et al., 2014) with a multisource data assimilation framework that incorporates both in situ and EO data. The dataset was generated using a complex modeling approach, a rigorous technical validation was needed to ensure its quality and reliability for subsequent analysis. Therefore, a comprehensive validation was performed separately at both point-scale in situ snow depth (HS) observation locations and across the 2D spatial domain using the satellite-retrieved SCA (Dall'Amico et al., 2025). More details on the data generation methodology and technical validation can be found in Dall'Amico et al. (2025).

3 Methodology

We evaluated 30 years of daily SWE time series data using a stratified random sampling approach to quantify changes in SWE across different elevation bands from 0 to 4500 m a.s.l. at an interval of 500 m. For each of the six elevation bands, 1000 random points were generated to extract their full 30-year daily SWE time series, a sampling strategy that ensures robust spatial representative coverage of topographic variability.

3.1 Snow phenology metrics

To assess changes in SWE dynamics over time, we selected six key snow phenology metrics for each hydrological water year. The metrics were selected based on their relevance in characterizing either snow water volume or snow duration. The three snow volume metrics include Maximum SWE (MaxSWE), April 1 SWE (April1SWE) (Mote et al., 2008) and Snow Water Storage (SwS) (Aragon and Hill, 2024), while, the snow duration metrics include SWE Duration (SWEduration), Day of Year of Max SWE (MaxSWE.dowy) and Snow Disappearance Date (SDD) (Gleason et al., 2019).

Maximum SWE (MaxSWE) represents the maximum value of SWE observed during a given water year (Jenicek et al., 2018). It is a fundamental indicator of the total volume of snow water storage within the seasonal snowpack just prior to the spring melt season (Jenicek et al., 2018). It represents an integrated summary of the weather in the previous winter, reflecting the snow accumulation and ablation processes providing a useful estimate of the potential runoff volume (Mote, 2006; Mote et al., 2018).

April 1 SWE is widely used as a conventional reference point for estimating peak snowpack in many mountain regions in the United States (Mote et al., 2008; Mote, 2006; Mote et al., 2018; Pederson et al., 2011). The SWE on April 1 was calculated due to its historical significance in the SWE measurements (Pederson et al., 2011). Furthermore, it is also used as an indicator of peak SWE in non-glacierised locations (Marty et al., 2023; Bohr and Aguado, 2001).

Snow Water Storage (SwS) (Aragon and Hill, 2024), defined as the integral of the SWE curve over time (length-time; m·d), characterizing the total seasonal volume of water stored in the snowpack (Aragon and Hill, 2024). Furthermore, unlike other snow metrics such as MaxSWE (static single point measure) or SWE duration (length of the snow season), SwS is applicable in both spatial and temporal scales (Aragon and Hill, 2024). This unique characteristic of SwS allows us to quantify snowpack storage and its long-term temporal changes (Aragon and Hill, 2024).

https://doi.org/10.5194/egusphere-2025-5520
Preprint. Discussion started: 18 December 2025

SWE Duration (Marty, 2008) quantifies the length of the persistent snow presence within a hydrological year. In this study, it is defined as the number of continuous days during each hydrological year when SWE exceeds 1 mm (Marty, 2008).

Day of year of Max SWE (MaxSWE.dowy) is the day of year on which the maximum SWE occurs. It is used to describe the onset of the snowmelt season (Jenicek et al., 2018; Marty et al., 2023).

Snow Disappearance Date (SDD) is defined as the first snow-free date after the peak SWE (Gleason et al., 2019; Smoot and Gleason, 2021). The SDD acts as a key indicator of snowmelt timing (Stone et al., 2002). It also influences the ecosystem by affecting the energy budget, determines the duration and timing of the growing season; it affects soil temperature due to the thermal insulation properties of snow (Edwards et al., 2007), and the reduction in the release of nutrients such as Nitrogen (Caron et al., 2025).

3.2 Trend analysis

To assess and compute long-term changes in the six selected snow phenology metrics, we applied the Mann-Kendall trend test (Mann, 1945; Kendall, 1962). It is a non-parametric statistical method widely used in environmental and hydrological studies to detect monotonic trends in time-series data (Yue et al., 2002). This method is very well suit*f*ed for environmental data, as it does not assume a specific distribution of the data and is robust to missing values and outliers (Hirsch et al., 1982). This makes it ideal for analyzing snow-related time series, which are often characterized by non-normality and occasional gaps.

In this study, the Mann-Kendall test was applied to the time series of each metric in different elevation bands. To assess the trends for each snow phenology metric-elevation combination, the test was applied to all the 1000 randomly selected points data for every elevation zone over the 30-year period (1991-2021). Trend detection and significance were calculated using the Kendall tau coefficient, while the statistical significance of trends was computed using the corresponding p values. A significance threshold of 0.05 was used to check whether a trend is statistically significant.

3.3 Basin-wide SWE volume calculation

We estimated the total volume of water stored in the SWE across the study domain expressed in Giga metric cube (Gm^3) by multiplying the daily SWE values at each pixel by the area of each pixel (500 x 500 m^2) and then all individual pixel volumes were summed across the entire study domain to obtain the total basin-wide SWE volume. This method provides an integrated estimate of basin-wide water storage in the snowpack, following the approach described by Avanzi et al. (2023).

3.3.1 Anomaly calculation

In order to assess long-term changes, we calculated the relative anomaly change for representative snow phenology metrics. We selected two from snow volume (peak SWE, April1 SWE), and two from snow duration (SWE duration and SDD) for different elevation bands. We first calculated the pixel-wise mean of each of these metrics for both reference (1991/1992 to 2010/2011) and recent periods (2011/2012 to 2020/2021). The elevation-wise change was calculated by taking the sum of all

https://doi.org/10.5194/egusphere-2025-5520
Preprint. Discussion started: 18 December 2025

pixels in both the reference and recent periods, and then the relative change as a percentage was computed based on these total sums using the following formula:

$$\left(\frac{\text{recent} - \text{reference}}{\text{reference}}\right) \times 100 \quad (1)$$

For snow duration metrics, we simply calculated the absolute difference (anomaly = recent_mean - reference_mean) in days.

4 Results

4.1 Total basin-wide SWE volume

The annual cycle of the total basin-wide SWE volume for the 30-year period (1992–2021) is shown in Fig. 2. The study domain shows a distinct and regular seasonal pattern of snow accumulation and melt across the basin. From the median niveograph, the maximum SWE volume reaches a magnitude of approximately 5.6 Gm^3 and typically occurs in mid-March (median DOY: 166). The timing of the peak is also variable, generally occurring between the end of February and early April. From the interquartile range (Q1–Q3), the range is wider around the time of peak SWE, showing that the largest interannual differences occur during the late winter. At the time of the median peak, the SWE volume for a typical year can range from 4.7 Gm^3 (25th percentile) to 7.2 Gm^3 (75th percentile).

Niveograph patterns diverge across the elevational gradient, where lower elevations demonstrate flashier more ephemeral snowpacks, and higher elevations demonstrate deep persistent snowpacks (Fig. 3) Fig. 3 shows the comparison of basin-wide SWE volume across different elevation bands, comparing the mean of the recent decade (2012-2021) with that of the reference baseline period (1992-2011). The interquartile range (Q1–Q3) of the reference period shows significant variability, which highlights the variability in SWE volume conditions at all elevations. All bands show the typical seasonal cycle of accumulation and melt, with the lower band (0-500 m) showing the ephemeral type of niveograph (Fig. 3). In the lower elevation bands (0-1500 m), a consistent SWE deficit can be observed in the mean SWE volume in the recent decade compared to the baseline, with smaller peaks and reduced snow durations (Fig. 3). From 1500-2000 m, the recent decade mean line is more or less close to the baseline, but during the accumulation and melt season, the recent decade mean is below the reference mean, indicating a clear but smaller in magnitude SWE deficit which is prominent with earlier melt onset (Fig. 3). From the lower to middle elevation bands (0-2000 m), the maximum SWE volume remained closer to the baseline, generally occurring from mid-February to early March (Fig. 3). In the higher elevation bands (2000–2500 m and 2500–4500 m), the SWE volumes were mainly higher than baseline conditions during the accumulation and melt periods but showed a more rapid decline in SWE compared to lower elevations (Fig. 3). The peak SWE volume typically occurred in early March for the 2000–2500 m band and in mid- to late-May for the 2500–4500 m band, aligning closely with the reference period.

https://doi.org/10.5194/egusphere-2025-5520
Preprint. Discussion started: 18 December 2025

4.2 Interannual and decadal variability

4.2.1 Inter-annual variability

The evolution of the SWE volume exhibits a strong, elevation-dependent pattern in both its accumulation and timing, as well as in its interannual variability (Fig. 4). In recent years, there is a clear general decrease in the volume of water across elevation bands and a shift of high SWE volumes to higher elevations with earlier melt-out (Fig. 4). Fig 4 shows the variability of the SWE volume using the time-elevation Hovmöller plot for each water year from 1991/1992 to 2020/2021. For each water year, these plots show the total elevation-wise SWE volume of water and the snow disappearance timing. All lower elevation bands (<1500 m) show more variable and generally lower SWE volumes, with earlier snowmelt timing and greater interannual variability (Fig. 4). In those elevations bands, the seasonal snow pack begins accumulating in December-January with peak volume in February for 0-1000 m and in March for 1000-1500 m. The snow disappearance shows a clear elevation-dependent pattern from the lower to higher elevation bands. For example, from 0-1000 m, the snow disappearance is by the end of March, whereas from 1000-1500 m is by the end of April and 1500-2000 m is by May (Fig. 4). All higher elevation bands (>2000 m) consistently accumulate SWE during the winter months (November-March), with maximum accumulation typically occurring in April and snow disappearance extending into the spring and early summer months (June-July) (Fig. 4). The middle elevation band (1500-2000 m) shows transitional characteristics between the lower and higher elevation bands.

The interannual variability is evident across all the elevation bands, with some years (e.g., WY2001, WY2009, WY2014) having high SWE volume across all the elevation bands, whereas the years (WY2005, WY2016, WY2017) show comparatively smaller SWE volume (Fig. 4). High-snow years such as 2008/2009 and 2012/2013 show both higher volume and delayed melt, whereas low-snow years like WY16 show low volumes and an earlier snow disappearance across all the elevation bands.

4.2.2 Decadal Variability

A consistent decline in volume of water from SWE is observed at lower elevations, indicating that regions below 1500 m are experiencing reduced snow accumulation over time (Table **??**). Table **??** shows the basin-wide decadal total volume of water available from SWE (Gm^3) for different elevation bands. In lower elevations the inter-decadal comparison shows an increase in volume from decade 1 to decade 2, followed by a significant decrease between decade 2 to decade 3 (Table **??**). For example, in lowest elevation (0–500 m), the total basin-wide volume of water first increases from 6.5 Gm^3 in 1991-2001 to 8.4 Gm^3 in 2002-2011 ($\sim$ 29% increase) and then declining substantially to 4.6 Gm^3 in 2012-2021 (45% decrease from decade 2). Overall, there is a decline of -29% between decade 1 and decade 3. Similarly, at 500–1000 m, the total available volume of water decreased from 49.4 Gm^3 (1991-2001) to 72.6 Gm^3 (2012-2021) (+46.9%), followed by a decrease to 38.6 Gm^3 (-46.8%) between decade 2 and 3. Overall, a decline of -22% between decade 1 and decade 3. The 1000–1500 m elevation zone also showed a notable decline (-23%) from 449.2 Gm^3 to 344.7 Gm^3 between decade 1 and decade 3. In 1000-1500 m band, the volume of water first increases from 449.2 Gm^3 in 1991-2001 to 514.8 Gm^3 in 2002-2011 (14% increase) and then shows a decline to 344.7 Gm^3 in 2012-2021 (33% decrease from decade 2). Overall, a decline of -23% is observed between decade 1 and decade 3 in elevation band 1000-1500 m. The 1500–2000 m elevation band experienced slight variations in

https://doi.org/10.5194/egusphere-2025-5520
Preprint. Discussion started: 18 December 2025

SWE, increasing from 1659.4 Gm^3 (1991-2001) to 1795.1 Gm^3 (2001-2011) (8% increase between decade 2 and 1), but then declining to 1622.3 Gm^3 in 2012-2021 (10% decrease between decade 1 and 3). Overall in 1500-2000 m band, there is a reduction of 2% between decade 1 and decade 3. The higher elevations (> 2000 m) exhibit opposite trend, with a decrease in volume from decade 1 to decade 2, followed by an increase between decade 2 to decade 3. At 2000–2500 m, the volume decreased from 3605.5 Gm^3 (1991-2001) to 3349.1 Gm^3 (2002-2011) (7% decrease) but then increased to 3817.8 Gm^3 (14% increase) in 2012-2021. Overall in 2000-2500 m band, there is a increase of 6% between decade 1 and 3. Similarly, at 2500–4500 m, the volume decreased from 3364.2 Gm^3 (1991-2001) to 2798.0 Gm^3 (2002-2011) (17% decrease between decade 1 and 2), but then increased to 3679.4 Gm^3 in 2012-2021 (31% increase between decade 2 and 3). Overall in >2500 m band, there is an increase of 9% between decade 1 and 3. These numbers show that the available volume of water from SWE in the study domain demonstrates a pronounced elevational gradient across all three decades. Additionally, the total basin-wide water exhibits complex trend over the study period. Decade 1 contained approximately 9134.2 Gm^3, and decade 2 has 8538.0 Gm^3 (-6.5% decrease between decade 1 and 2), whereas the decade 3 recorded 9507.4 Gm^3 (+11.4% from decade 2) with an overall increase of about 4% from between decade 1 and decade 3.

4.3 Temporal analysis of seasonal snow dynamics

The timing of the peak SWE and its disappearance show a strong elevation dependent pattern and significant interannual variability (Fig. 5 and 6). At lower elevations (0-1000 m), the peak SWE generally occurred in midwinter (January–February), March–May at mid elevations (1000-2000 m), and April-May at higher elevations (>2000 m). The timing of the peak SWE also shows interannual variability in all elevation bands. Indeed, compared to March 6 (assumed to be the median peak SWE date in Italy (Aragon and Hill, 2024)), indicated by the dashed line, some years highlight consistent patterns: lower elevations had peak dates clustered in January–February, mid elevations (1000–2000 m) predominantly peaked around February–March, and high elevations (2000–4500 m) exhibited peaks consistently from March onward.

The snow disappearance dates across different elevation bands for all water years from WY1992 to WY2021 show strong elevation-dependent and interannual variability (Fig. 6). Generally, snow disappeared earliest in lower elevation bands (0–500 m and 500–1000 m), typically by mid- to late spring (April–May). In contrast, higher elevation bands (>2000 m) exhibited snow persistence until late spring or early summer (June–July), indicating a clear elevation gradient in snow persistence. SDD also shows significant interannual variability, with certain years such as WY1999, WY2016, WY2017 showing earlier snow disappearance at all elevations, while years like WY1997, WY2001, WY2019 show late snow disappearance. High snow years (cf. Figure 4) generally show later snow disappearance dates at all elevations. In contrast, years with small and shallow snowpacks show earlier and more rapid snow disappearance dates.

4.4 Snow phenology metrics

The snowpack characteristics from both snow volume and snow duration for the study period exhibit a strong relationship with elevation (see supplementary Table S1). The mean annual (Max SWE) ranges from 8.8 mm/day in the lowest elevation band (0–500 m) to 742.6 mm eq. of water in the highest band (2500–4500 m). Similarly, mean April 1 SWE, an indicator of water

https://doi.org/10.5194/egusphere-2025-5520
Preprint. Discussion started: 18 December 2025

resource management (Mote, 2006), ranges from 0 mm at low elevations to 591 mm at higher elevations. Furthermore, the variability also exhibits a relationship with elevation. The standard deviation of Max SWE is 13.2 mm at 0-500 m but increases to 335.0 mm at 2500-4500 m, highlighting the much larger interannual variations in SWE volume at higher elevation bands. April 1 SWE standard deviations range from 0.1 to 283.2 mm in the highest elevation bands. SwS also exhibited the elevational dependence, with mean values ranging from 886.4 mm-day at 0-500 m to more than 26 million mm-day at 2500-4500 m.

The snow duration metrics also follow a clear elevation dependent pattern, similar to the snow volume metrics. The length of the snow season (SWEduration) is shortest at lowest elevations (averaging 5.0 days at 0-500 m) and longest at the highest elevations (254 days). The standard deviation in snow duration was relatively consistent in middle elevations (26 to 42 days), but decreased at the highest elevation (16 days). The timing of peak SWE occurrence (MaxSWE.dowy) on average per water year ranges from 81 days (late December) at 0-500 m to 210.0 days (late April) at 2500-4500 m, indicating later peak accumulation at higher elevations. The middle elevation zones (1000-2000 m) showed an intermediate timing of around 150 days (late February). Similarly, the SDD advances from from 83 days (late December) at 0-500 m to 258 days (mid-June) at 2500-4500 m. At the high elevations, the timing of snow persistance is more consistent, with the standard deviation of SDD decreasing from 51 days in the lowest band to 12 days in the highest band.

4.5 Trends in snow phenology metrics across different elevation bands

The snow phenology metrics representing snow volume and snow duration across the 30-year study period are shown in Table 2 and Fig. 7. Our results show strong elevation dependent trends across the study domain. This pattern is consistent across both snow volume metrics (Max SWE, April1SWE, SwS) and snow duration metrics (SWEduration, MaxSWE.dowy and SDD). The detailed statistical analysis for these key snow phenology metrics across different elevation bands are shown in Table 2 and Fig. 7.

4.5.1 Changes in snow volume storage

All snow volume metrics (max SWE, April1SWE and SwS) show strong negative trends throughout the 30-year study period, demonstrating overall losses in snow-water storage across the lowest elevations (0-1500 m a.s.l.) with very high p-values ($p < 10^{-}10$). The max SWE showed a strong decreasing trend (e.g., from Z = –32.0 at 0–500 m to Z = -7.30 at 1000-1500 m), showing a significant (τ = –0.13 at 0–500 m to τ = -0.02 at 1000-1500 m) reduction in maximum snow accumulation over time. From 0 to 1500 m, the decline continues but gradually weakens, and then a transition occurs from 1500-2000 m elevation band where the trend reverses to increasing (Z = 5.0895, τ = 0.01994) and reaches its maximum positive value in the highest elevation band (Z = 22.07, τ = 0.09). April1SWE, an important metric that traditionally represents snow conditions at the beginning of the ablation period, also shows a significant decline in the lowest elevations (Z = -3.86, τ = -0.02 at 0-500 m), with increasingly negative trends throughout the mid-elevations (Z = -10.13, τ = -0.05 at 500-1000 m). Similarly to Max SWE, a reversal occurs at 1500-2000 m (Z = 10.36, τ = 0.04), but the magnitude of positive change at higher elevations is significant, reaching Z = 33.85 with τ = 0.13 at 2500-4500 m. SwS, another snow volume metric, shows consistently strong decreasing trends in lower elevations. The trend remains negative, but weakens considerably at 1500-2000 m (Z = -3.86, τ =

https://doi.org/10.5194/egusphere-2025-5520
Preprint. Discussion started: 18 December 2025

-0.02), before reversing to increasing trend at 2000-2500 m (Z = 9.82, τ = 0.04) and further strengthening at 2500-4500 m (Z = 19.09, τ = 0.08). This pattern shows that snow water storage is significantly reducing at elevations below 2000 m and increasing at the highest elevations over the study period.

4.5.2 Snow duration metrics

The snow duration metrics (SWEduration, MaxSWE.dowy and SDD) show decreasing trends in most cases across all the elevations with a few exceptions at higher elevations. SWEduration shows persistent decreasing trends that extend up to 2500 m elevation, but in the highest elevation band, the trend increases, though relatively weak (Z = 3.64, τ = 0.01). This shows a widespread shortening of the snow seasons in most of the elevation bands. Like other metrics, MaxSWE.dowy does not follow a consistent relationship with elevation. In the 0-500 m elevation band, a decreasing trend was found suggesting an earlier peak snow accumulation. However, this shifts to an increasing trend at 500-1000 m (Z = 4.83, τ = 0.02), before changing back to decreasing trends at mid-to-high elevations, reaching higher values at 2000-2500 m (Z = -22.52, τ = -0.09). At the highest elevations (2500-4500 m), the trend remains negative but comparatively smaller (Z = -11.11, τ = -0.04). These changes in MaxSWE.dowy imply that the peak SWE is being reached earlier, even as if snow volume is increasing. SDD, an important metric that represents the end of the seasonal snow period is the only metric that shows a non-significant result in any elevation band (Z = -1.18, τ = -0.004, p = 0.2378 at 500-1000 m). At the lowest elevations (0-500 m), the SDD shows decreasing trend (Z=-5.33, τ=-0.02), indicating earlier snow disappearance. This decreasing trend strengthens considerably at 1000-1500 m (Z = -13.09, τ = -0.05) and 1500-2000 m (Z = -14.85, τ = -0.06) before changing to increasing trend at 2000-2500 m (Z = 3.36, τ = 0.01). The delayed SDD compared to Max SWE suggests that even when snow accumulation is increasing, the timing of complete snowmelt may not be proportionally delayed, pointing to potentially accelerated melt rates even at high elevations.

4.6 Long-term changes: Anomaly patterns

Our analysis shows profound changes in the SWE volume and its timing over the last 30 years (see Figs. 8 and 9). By comparing the recent decade (2012-2021) with the reference period (1992-2011), we found strong elevation-dependent patterns, such as low-to-mid elevations (<2000 m) are experiencing a loss of snow, while the highest elevations (>2000 m) are gaining (see Figs. 8 and 9). Furthermore, our results show that the main driver of the shrinking snow season is a delayed onset of snow in autumn. The following sections detail these changes in total snow-water storage, the magnitude of SWE, and its timing (Figs. 8 and 9).

4.6.1 Long-term losses in snow-water storage in the Italian Alps

During the past 30 years, the snow-water storage has changed differentially across all the elevation bands (8. The analysis of long-term changes in the total SWE volume for the period (1991-2021) is shown as the relative change (%) in the recent decade with reference to the mean of the first two decades (8. The results show a strong decrease in the total SWE volume. At lowest elevation (0-500 m), a substantial decrease of 38.0% was recorded. This decrease continues through mid-elevations, with a reduction of 36.6% at 500-1000 m and 28.5% at 1000-1500 m. In the 1500-2000 m elevation band, a smaller but notable

https://doi.org/10.5194/egusphere-2025-5520
Preprint. Discussion started: 18 December 2025

decrease of 6.1% was recorded. However, in the higher elevation bands (>2000 m), an increase in total volume of water was recorded. In the 2000-2500 m band, a moderate increase of 9.8% was recorded, while in the highest elevation band (2500-4500 m), an increase of 19.4% was recorded.

4.6.2 Changes in snowpack magnitude: peak SWE and April 1 SWE anomaly

The analysis of the peak SWE and April 1 SWE were used as an estimate of the amount of water available at the end of the snow season. The analysis of these key SWE dates (peak SWE and April 1 SWE) showed strong reductions at lower elevations (0-1500 m) (Fig. 9). Their pattern is nearly identical, with severe losses at low-to-mid elevations in both dates.

At the lowest elevations (0-500 m), the peak SWE shows a reduction of 91.6%. The decline continues, such as at 500-1000 m, there is a reduction of 55.6% and at 1000-1500 m, a reduction of 26.4% was recorded. In 1500-2000 m band, a small reduction of about 4% was recorded. However, at higher elevations (> 2000 m), an increase in peak SWE was recorded. In the bands 2000-2500 m and 2500-4500 m, a moderate increase of about 10% and 17% was recorded, respectively. For April 1 SWE, the pattern is nearly similar, with strong losses at lower elevations (-100 to -15.8% in the 0-1500 m band) and an increase at mid to high elevations (1500-4500 m), i.e., about 3 to 18%. These results highlight that the entire end-of-winter snowpack, not just on one specific date, is following this strong elevation-dependent pattern. For the dates, the spatial map (see Fig. 9) clearly shows the widespread losses in the lower valleys (red) and the gains in the highest mountain regions (blue). Furthermore, both dates reveal an elevational threshold around 1500 meters (see Fig. 9), where the SWE trend vary from strongly negative to positive.

4.6.3 Changes in snow season timing: Snow duration and SDD anomaly

The snow season timing analysis also shows an elevation-dependent pattern that complements the SWE magnitude changes (Fig. 9C). In lower elevations (0-1500 m), there is a significant reduction in snow season, with the most severe impacts at 1000-1500 m showing an average loss of 20.8 days. However, at the lowest elevations (<1000 m), a slight to moderate decrease of -1.2 to -6.3 days was observed. The highest elevations (>2500 m) show a modest increase in the duration of snow, gaining up to +5.1 days.

The long-term analysis of SDD shows comparatively much smaller changes (Fig. 9D). At the lowest elevations, the SDD occurs slightly later (+7.2 days) than in the reference period. Mid-elevations (500-1500 m) show a moderately earlier SDD of 2.3 to 2.4 days, while higher elevations show delayed melt-out, with the 2500-4500 meter band showing a 2.4 day delay. These results highlight that the primary driver for the shorter snow season is the later onset of snow in the autumn, because the small reduction (-2.3 days in the 1000-1500 m band) cannot account for the massive 21 day loss in duration (see Fig. 9C).

4.6.4 Winter months anomaly

Analysis of monthly SWE anomalies in winter months (December, January, February, and March) shows strong elevation-dependent changes between the recent decade (2012-2021) and the reference decades (1992-2011) (Fig. 10). There is a consistent delay in the onset of snow at very low elevations (0-1000 m). In the lower elevations (0-1500 m) bands, we found

https://doi.org/10.5194/egusphere-2025-5520
Preprint. Discussion started: 18 December 2025

consistent negative anomalies (reduced SWE) across all the winter months. This delay is most pronounced in December, January and February, which strongly indicates that early winter accumulation is being impacted by either delayed snowfall or a shift in precipitation from snow to rain.

For all winter months, there is a clear transition around the 1500-2000 m elevation band, consistent with our previous results (see section 4.5.1). In this band, there is also comparatively more variability than in the lower elevation bands, as shown by the spread of the data (Fig. 10). In the higher elevations (> 2500 m), there is a clear increase in winter SWE. This positive anomaly grows progressively from December to March, with the largest gains in SWE occurring in late winter. In this band, the variability also increases substantially at higher elevations.

4.7 Comparison with other dataset

In the absence of comprehensive reference spatial SWE data in the study domain, we made a comparison of our dataset (hereafter, WaterJade for comparison) with another similar (but shorter) SWE dataset called IT-SNOW (Avanzi et al., 2023). IT-SNOW is a snow reanalysis data for the whole of Italy and is available as daily 500 m spatial resolution maps of SWE, HS, bulk snow density (RhoS), and liquid water content (Theta_W) (Avanzi et al., 2023). For comparison, we used the variable SWE from IT-SNOW. The data were then reprojected, masked to WaterJade dataset, and temporarily aligned to a common time period (2011-2021). Then we computed the daily total SWE volume (Gm^3) for the study domain from both datasets (Fig. 11). Furthermore, for elevation-dependent analysis, we also calculated the daily SWE volume within each elevation band from both the datasets (Fig. 12). A comparison of the daily basin-wide SWE volume for the 2011–2021 period shows a strong overall agreement between WaterJade dataset and the IT-SNOW dataset (Fig. 11). Both datasets are able to capture the timing and magnitude of seasonal snow accumulation and melt, while WaterJade dataset shows slightly higher peak volumes than IT-SNOW data with R^2 = 0.87, RMSE = 0.81 Gm^3 and MAE = 0.58 Gm^3, indicating strong overall agreement between the two datasets. Furthermore, an elevation-wise comparison shows that there is a large difference at lower elevations (0-500 m, R^2 = 0.31; 500-1000 m, R^2 = 0.45), where IT-SNOW generally shows higher SWE volume during peak accumulation, whereas WaterJade dataset shows slightly higher volume in higher elevations (>2000 m) (Fig. 12). However, in the middle elevation band (1500-2000 m), both the datasets show a very strong correlation (R^2 = 0.91) (Fig. 12). This could be due to the good number of in situ data forcings available in this elevation band. For the period 2010 to 2021, the basin-wide SWE volume from WaterJade dataset was 4.0 Gm^3 and 3.49 Gm^3 from the IT-SNOW product (Avanzi et al., 2023).

5 Discussion

This study presents a comprehensive climatology of the long-term (1991-2021) SWE dataset (Dall'Amico et al., 2025) in the Po River Basin, Italy, providing key information on the response of seasonal snowpack to ongoing climate warming (Avanzi et al., 2024; Colombo et al., 2023; Koehler et al., 2022). Our results show profound losses across the study area except for the highest peaks (see Fig. 8). Our results also demonstrate (see our initial hypothesis Fig. 13) pronounced elevation-dependent changes, with key changes observed across low- and mid-elevation zones (see Table 2 and Fig. 8). We found that low-to-mid

https://doi.org/10.5194/egusphere-2025-5520
Preprint. Discussion started: 18 December 2025

elevation zones (<2000 m) are experiencing pronounced declines in both snow volume and duration (see Fig. 9). In contrast, high-elevation zones (>2500 m) are experiencing increased accumulation, but a continued shortened snow season (see Fig. 7). This elevation-dependent changes and loss of the seasonal snowpack highlight a fundamental shift in the hydrological regime of the Po River Basin, with significant implications for the timing and volume of runoff and the future availability of water in the region (Aragon and Hill, 2024; Avanzi et al., 2024; Colombo et al., 2023).

5.1 SWE changes

The profound interannual variability in SWE as shown in Figures 4 and 11 is due to spatial variability and elevation gradients in temperature and precipitation patterns, which collectively control the snow accumulation and melt processes (Clark et al., 2011). Large-scale weather patterns further affect this variability by controlling the temperature and transport of moisture (Beniston, 1997). For example, during the 2021-2022 snow drought (Avanzi et al., 2024), a persistent anticyclonic anomaly was observed in western Europe (Faranda et al., 2023).

The findings of this study show different threshold elevations for different snow phenology metrics, such as, Max SWE: 1500 m, April 1st SWE: 1500 m, SwS: 2000 m, SWE Duration: 2500 m, MaxSWE.dowy: Complex pattern, SDD: 2000 m. However, the key finding is not a single, precise threshold but rather the consistent pattern that SWE volume and persistence are declining across all low- to mid-elevation zones. This general pattern aligns with broader projections for the Alps, which anticipate a decrease in snow cover below 1500-2000 m(Gobiet et al., 2014). These threshold elevations will have strong implications for water management (Beniston et al., 2018) in the study domain, as highlighted by recent snow droughts (Avanzi et al., 2024; Colombo et al., 2023). Generally, higher elevation thresholds for snow duration metrics compared to SWE volume metrics suggest that snow seasons are shortening even in zones where maximum snow accumulation is increasing. However, increasing snow accumulation at higher elevations should be taken with caution, because ERA5 systematically overestimates high elevation precipitation in the Alps (Bandhauer et al., 2022). The reduction in snow duration agrees with the results of Carrer et al. (2023), who mentioned a shorter snow duration of 36 days based on tree-ring width records.

The consistency and magnitude of the declining trends across different snow phenology metrics (Table 2) highlight the robustness of these patterns despite natural interannual variability, model uncertainty, input bias, etc. Our results highlight that the loss of SWE volume and changes in melt-timing in mountain hydrology will likely intensify with continued global warming (IPCC, 2023; Huss et al., 2017), with disproportionate impacts on lower to mid-elevation zones that historically relied on seasonal snow pack for water. Our findings are also consistent with other recent studies in the Alps, for example, Matiu et al. (2021) reported similar reductions in snow depth, and Bozzoli et al. (2024) also linked such declines to changes in regional snowfall patterns.

5.2 Role of increasing temperatures and phase change of precipitation

An increase in air temperatures worldwide (Kotlarski et al., 2022; IPCC, 2023) is directly related to a change in the phase of precipitation from solid to liquid (Viviroli et al., 2011; Beniston et al., 2018), leading to an upward shift of the elevation of snowline (Beniston et al., 2018). Rising temperatures can have a significant effect in locations close to freezing level (Beniston

https://doi.org/10.5194/egusphere-2025-5520
Preprint. Discussion started: 18 December 2025

et al., 2018), and our results clearly show the direct effect of these changes in the Po River Basin (see Fig. 8). Long-term declining trends in both SWE volume and its duration (see Fig. 9), particularly at lower to mid elevations (0-2000 m), can be directly linked to an increase in air temperatures and changes in the precipitation phase. Our results further suggest that the reduction in snow duration is driven by a delayed onset of snow accumulation (see Fig. 10). Furthermore, rising spring temperatures increase the rate of snowmelt (Stewart, 2009). The accelerated melt is evident in the earlier snow disappearance dates across all elevation bands (see Fig. 6). This observed decline in SWE volume, changes in melt timing, and accelerated melt patterns directly influence the magnitude and timing of seasonal runoff, impacting the hydrological regime of the study region. Other studies show congruent results in the region (Avanzi et al., 2024; Colombo et al., 2023, 2022; Bozzoli et al., 2024; Marcolini et al., 2017).

5.3 Implications for water management in Po River Basin

The long-term climatology of SWE shows a significant decrease in the volume of water from the seasonal snowpack (see Fig. 7), with changes occurring in both the accumulation and ablation patterns. This decline will have significant implications for the availability of water in the Po River Basin, which historically has a large contribution of about 50% (Avanzi et al., 2023) from snowmelt. Earlier snow disappearance, particularly at low and mid-elevations (see Figures 8 and 7), directly translated into an earlier onset of peak spring streamflow. This behavior changes the hydrographs of mountain rivers and, in turn, leads to reduced water availability during the typically drier late spring and summer months (Coppola et al., 2014) when the water demand for agriculture, domestic use, and hydropower is at its peak (Viviroli et al., 2007). Furthermore, changes in snowpack volume and melt-out timing increase the risk of floods (Blöschl et al., 2019) and snow droughts (Avanzi et al., 2024; Huning and AghaKouchak, 2020). This fundamental shift towards a lower, earlier and more uncertain runoff regime underscores that a critical reassessment of existing water management practices, reservoir management, and irrigation timing is needed. This is also supported by other studies regarding the Po River District (Coppola et al., 2014; Avanzi et al., 2024) as well as by the LIFE ClimaxPo project started in 2023 and led by the Po River District Basin Authority (LIFE CLIMAX PO Project, 2023).

5.4 Limitations and future research

The present study highlights key insights into the long-term dynamics of SWE in the Po River Basin, Italy. At the same time, it is also important to acknowledge some limitations and biases in this dataset, mostly in the higher elevations of the study domain. This SWE dataset despite being generated from a comprehensive methodology (Dall'Amico et al., 2018, 2025), needs in situ meteorological forcings as input to the model, but are sparse in high mountainous terrain (Viviroli et al., 2011; Shahgedanova et al., 2021). Therefore, in the generation of this dataset ERA5-Land data was used as input wherever in situ data were not available (Dall'Amico et al., 2025) carrying biases that can propagate directly into the final SWE estimates, particularly in higher elevations where meteorological stations are sparse, as described in the following subsection.

https://doi.org/10.5194/egusphere-2025-5520
Preprint. Discussion started: 18 December 2025

5.4.1 Elevation-dependent changes and precipitation bias

The 30-year analysis shows dramatic decreases in snow water storage at lower elevations: 38.0% reduction at 0-500 m, 36.6% at 500-1000 m, and 28.5 % at 1000-1500 m (Fig. 8). In contrast, the highest elevations (2500-4500 m) show an increase of 10-20%. However, the increase in snow water storage at high elevations requires careful interpretation due to methodological constraints (Hersbach et al., 2020; Muñoz-Sabater et al., 2021). Ground-based meteorological stations are sparse at high elevations (Viviroli et al., 2011; Shahgedanova et al., 2021), necessitating the incorporation of reanalysis datasets like ERA5-Land (Muñoz-Sabater et al., 2021) for model forcings. Based on the Global Historical Climatology Network-Monthly (GHCN-M) Lawrimore et al. (2011); Mountain Research Initiative EDW Working Group (2015), globally less than 1% of in situ stations are located over 3000 m a.s.l. and only 3% are above 2000 m a.s.l. Subsequent validation of ERA5/ERA5-Land likely overestimates high-elevation precipitation (Dalla Torre et al., 2024; Monteiro and Morin, 2023; Bandhauer et al., 2022; Shrestha et al., 2023) and should be used with caution (Jiao et al., 2021), potentially creating artificial increases in the modeled snow accumulation above 1500 m (Hersbach et al., 2020). This is due to the single layer snow parameterization available in both ERA5 and its subsidiary ERA5-Land, which does not produce enough melting (Hersbach et al., 2020; Muñoz-Sabater et al., 2021). The wet bias is particularly concerning as independent glaciological studies suggest actual glacier retreat and ice losses at higher elevations (Sommer et al., 2020; Hock et al., 2019). The discrepancy highlights fundamental challenges in mountain hydrology, where the impacts of climate change may be more pronounced, but observational data are the scarcest (Mountain Research Initiative EDW Working Group, 2015). The systematic overestimation of high elevation precipitation by ERA5/ERA5-Land requires careful validation and bias correction for mountain hydrological studies (Dalla Torre et al., 2024).

To overcome these limitations, the present study underscores the need for an increase in the high elevation meteorological network with more variables, as highlighted by Viviroli et al. (2011); Mountain Research Initiative EDW Working Group (2015). Furthermore, the integration of active remote sensing methods such as interferometric synthetic aperture radar (InSAR) would be useful for the reconstruction of high-resolution SWE as shown by Premier et al. (2023); Oveisgharan et al. (2024) and application of cosmic-ray neutron sensing (CRNS) for the estimation of SWE over large areas (Schattan et al., 2019). The next remote sensing mission such as NASA-ISRO Synthetic Aperture Radar (NISAR) could be a game changer for the retrieval of SWE with a repeat pass of 12 days and a resolution of 3-10 m^2 (https://nisar.jpl.nasa.gov/mission/quick-facts/). Additionally, continuous model development and refinement of physically-based snow models, coupled with data assimilation techniques are essential for reducing uncertainties in high-resolution SWE generation.

6 Conclusions

In this study, a comprehensive analysis of long-term (30-year) snow water equivalent dataset was performed in the mountain part of the Po River District, Italy, consisting of parts of the Alps and Apennines from 1991 to 2021. Our results show a clear, elevation-dependent pattern with profound losses at lower elevations. The primary driver of this loss is a clear rise in air temperatures that mainly affects the 0–1500 m zone.

https://doi.org/10.5194/egusphere-2025-5520
Preprint. Discussion started: 18 December 2025

All snow volume metrics peak SWE, April1SWE and snow water storage show substantial decline across lower elevations (0-1500 m), representing a significant loss in total water storage capacity of the study region. However, snow duration metrics show a shorter snow season across nearly all elevations with a few exceptions at higher elevations. Furthermore, long-term analysis show significant changes in both the magnitude of SWE and its timing in different elevation bands. For example, in the recent decade (2011-2021), there has been a decrease in snow duration of about 20 days in the 1000 to 1500 m band. And in volume of water, at the lowest elevation (0-500 m), a substantial decrease of 38.0% was observed. This decrease continues through mid-elevations, with a reduction of 36.6% at 500-1000 m and 28.5% at 1000-1500 m. Our results also show that in the 0-2000 m elevation bands, there are consistent negative SWE anomalies in the months of December, January, and February. Even in the month of March, a negative anomaly can be found from 0-1500 m. This delay in persistent snow onset, loss of snow volume marks a fundamental shift in the hydrological regime of the study region. Therefore, our results show that there is a transition from a historically stable snowpack to more variable and uncertain snow dynamic patterns in the Po River Basin. The combined effect of this profound loss of snow-water storage at low elevations and the earlier, more rapid disappearance of the snowpack will have significant implications for regional hydrology and water resource management, signaling a fundamental change in the timing and volume of runoff.

Code and data availability. The SWE dataset is freely available as GeoTIFF files on the repository: https://doi.org/10.5281/zenodo.11196628 and is distributed under Creative Commons Attribution 4.0 International license: https://creativecommons.org/licenses/by/4.0/

.

Author contributions. Conceptualization (All Authors), Writing - Original draft (JMW), Methodology (JMW, KG, RR), Writing – review and editing (All Authors), Funding acquisition (RR,MB,FT), Formal analysis (JMW, KG), Visualisation (JMW, KG, RR), Data collection (MD, FP, ST, GR, MB, FT). All the authors contributed in editing and reviewing the manuscript.

Competing interests. All the authors declare that they have no conflict of interest.

Acknowledgements. The work of JMW has been funded by Fondazione CARITRO Cassa di Risparmio di Trento e Rovereto, grant number 2022.0246. RR and JMW would like to thank and acknowledge the funding from the European Union under NextGenerationEU. PRIN 2022 Prot. n. 202295PFKP project. KG would like to thank and acknowledge the USA and Italy Fulbright Scholars Fellowship.

https://doi.org/10.5194/egusphere-2025-5520
Preprint. Discussion started: 18 December 2025

References

Abegg, B., Agrawala, S., Crick, F., and Montfalcon, A. d.: Climate change impacts and adaptation in winter tourism, in: Climate Change in the European Alps, edited by Agrawala, S., Organization for Economic Co-operation and Development (OECD), Paris Cedex, France, 2007.

ADBPO: Caratteristiche del Bacino del Fiume Po e Primo Esame dell' Impatto Ambientale Delle Attivitá Umane Sulle Risorse Idriche (Characteristics of the Po River Basin and First Examination of the Environmental Impact of Human Activities on Water Resources) (In Italian), Tech. rep., https://www.adbpo.it/download/bacino_Po/, 2006.

Aragon, C. M. and Hill, D. F.: Changing snow water storage in natural snow reservoirs, Hydrol. Earth Syst. Sci., 28, 781–800, https://doi.org/10.5194/hess-28-781-2024, 2024.

Avanzi, F., Gabellani, S., Delogu, F., Silvestro, F., Pignone, F., Bruno, G., Pulvirenti, L., Squicciarino, G., Fiori, E., Rossi, L., Puca, S., Toniazzo, A., Giordano, P., Falzacappa, M., Ratto, S., Stevenin, H., Cardillo, A., Fioletti, M., Cazzuli, O., Cremonese, E., Morra di Cella, U., and Ferraris, L.: IT-SNOW: a snow reanalysis for Italy blending modeling, in situ data, and satellite observations (2010–2021), Earth Syst. Sci. Data, 15, 639–660, https://doi.org/10.5194/essd-15-639-2023, 2023.

Avanzi, F., Munerol, F., Milelli, M., Gabellani, S., Massari, C., Girotto, M., Cremonese, E., Galvagno, M., Bruno, G., Morra di Cella, U., Rossi, L., Altamura, M., and Ferraris, L.: Winter snow deficit was a harbinger of summer 2022 socio-hydrologic drought in the Po Basin, Italy, Communications Earth & Environment, 5, 1–12, https://doi.org/10.1038/s43247-024-01222-z, 2024.

Bandhauer, M., Isotta, F., Lakatos, M., Lussana, C., Båserud, L., Izsák, B., Szentes, O., Tveito, O. E., and Frei, C.: Evaluation of daily precipitation analyses in E-OBS (v19.0e) and ERA5 by comparison to regional high-resolution datasets in European regions, Int. J. Climatol., 42, 727–747, https://doi.org/10.1002/joc.7269, 2022.

Beniston, M.: Variations of snow depth and duration in the Swiss alps over the last 50 years: Links to changes in large-scale climatic forcings, Clim. Change, 36, 281–300, https://doi.org/10.1023/A:1005310214361, 1997.

Beniston, M., Farinotti, D., Stoffel, M., Andreassen, L. M., Coppola, E., Eckert, N., Fantini, A., Giacona, F., Hauck, C., Huss, M., Huwald, H., Lehning, M., López-Moreno, J.-I., Magnusson, J., Marty, C., Morán-Tejéda, E., Morin, S., Naaim, M., Provenzale, A., Rabatel, A., Six, D., Stötter, J., Strasser, U., Terzago, S., and Vincent, C.: The European mountain cryosphere: a review of its current state, trends, and future challenges, Cryosphere, 12, 759–794, https://doi.org/10.5194/tc-12-759-2018, 2018.

Blöschl, G., Hall, J., Viglione, A., Perdigão, R. A. P., Parajka, J., Merz, B., Lun, D., Arheimer, B., Aronica, G. T., Bilibashi, A., Boháč, M., Bonacci, O., Borga, M., Čanjevac, I., Castellarin, A., Chirico, G. B., Claps, P., Frolova, N., Ganora, D., Gorbachova, L., Gül, A., Hannaford, J., Harrigan, S., Kireeva, M., Kiss, A., Kjeldsen, T. R., Kohnová, S., Koskela, J. J., Ledvinka, O., Macdonald, N., Mavrova-Guirguinova, M., Mediero, L., Merz, R., Molnar, P., Montanari, A., Murphy, C., Osuch, M., Ovcharuk, V., Radevski, I., Salinas, J. L., Sauquet, E., Šraj, M., Szolgay, J., Volpi, E., Wilson, D., Zaimi, K., and Živković, N.: Changing climate both increases and decreases European river floods, Nature, 573, 108–111, https://doi.org/10.1038/s41586-019-1495-6, 2019.

Bohr, G. S. and Aguado, E.: Use of April 1 SWE measurements as estimates of peak seasonal snowpack and total cold-season precipitation, Water Resources Research, 37, 51–60, https://doi.org/10.1029/2000WR900256, 2001.

Bonnell, R., McGrath, D., Tarricone, J., Marshall, H.-P., Bump, E., Duncan, C., Kampf, S., Lou, Y., Olsen-Mikitowicz, A., Sears, M., Williams, K., Zeller, L., and Zheng, Y.: Evaluating L-band InSAR snow water equivalent retrievals with repeat ground-penetrating radar and terrestrial lidar surveys in northern Colorado, Cryosphere, 18, 3765–3785, https://doi.org/10.5194/tc-18-3765-2024, 2024.

https://doi.org/10.5194/egusphere-2025-5520
Preprint. Discussion started: 18 December 2025

Bozzoli, M., Crespi, A., Matiu, M., Majone, B., Giovannini, L., Zardi, D., Brugnara, Y., Bozzo, A., Berro, D. C., Mercalli, L., and Bertoldi, G.: Long-term snowfall trends and variability in the Alps, Int. J. Climatol., https://doi.org/10.1002/joc.8597, 2024.

Brown, R. D.: Northern hemisphere snow cover variability and change, 1915–97, J. Clim., 13, 2339–2355, https://doi.org/10.1175/1520-0442(2000)013<2339:NHSCVA>2.0.CO;2, 2000.

Caron, S. B., Campbell, J., Driscoll, C. T., Groffman, P. M., Leonardi, B., Reinmann, A., Rustad, L., Wilson, G., and Templer, P. H.: Shallow snowpack and early snowmelt reduce nitrogen availability in the northern hardwood forest, Biogeochemistry, 168, 1–20, https://doi.org/10.1007/s10533-025-01239-2, 2025.

Carrer, M., Dibona, R., Prendin, A. L., and Brunetti, M.: Recent waning snowpack in the Alps is unprecedented in the last six centuries, Nat. Clim. Chang., 13, 155–160, https://doi.org/10.1038/s41558-022-01575-3, 2023.

Chartier-Rescan, C., Wood, R. R., and Brunner, M. I.: Snow drought propagation and its impacts on streamflow drought in the Alps, Environ. Res. Lett., 20, 054 032, https://doi.org/10.1088/1748-9326/adc824, 2025.

Clark, M. P., Hendrikx, J., Slater, A. G., Kavetski, D., Anderson, B., Cullen, N. J., Kerr, T., Örn Hreinsson, E., and Woods, R. A.: Representing spatial variability of snow water equivalent in hydrologic and land-surface models: A review: REPRESENTING SPATIAL VARIABILITY OF SWE IN MODELS, Water Resour. Res., 47, https://doi.org/10.1029/2011WR010745, 2011.

Colombo, N., Valt, M., Romano, E., Salerno, F., Godone, D., Cianfarra, P., Freppaz, M., Maugeri, M., and Guyennon, N.: Long-term trend of snow water equivalent in the Italian Alps, J. Hydrol. (Amst.), 614, 128 532, https://doi.org/10.1016/j.jhydrol.2022.128532, 2022.

Colombo, N., Guyennon, N., Valt, M., Salerno, F., Godone, D., Cianfarra, P., Freppaz, M., Maugeri, M., Manara, V., Acquaotta, F., Petrangeli, A. B., and Romano, E.: Unprecedented snow-drought conditions in the Italian Alps during the early 2020s, Environ. Res. Lett., 18, 074 014, https://doi.org/10.1088/1748-9326/acdb88, 2023.

Copernicus, C. S.: Global Climate Highlights 2024, https://climate.copernicus.eu/global-climate-highlights-2024, accessed: 2025-5-19, 2025.

Coppola, E., Verdecchia, M., Giorgi, F., Colaiuda, V., Tomassetti, B., and Lombardi, A.: Changing hydrological conditions in the Po basin under global warming, Sci. Total Environ., 493, 1183–1196, https://doi.org/10.1016/j.scitotenv.2014.03.003, 2014.

Dalla Torre, D., Di Marco, N., Menapace, A., Avesani, D., Righetti, M., and Majone, B.: Suitability of ERA5-Land reanalysis dataset for hydrological modelling in the Alpine region, J. Hydrol. Reg. Stud., 52, 101 718, https://doi.org/10.1016/j.ejrh.2024.101718, 2024.

Dall'Amico, M., Endrizzi, S., and Tasin, S.: Mysnowmaps: operative high-resolution real-time snow mapping, in: International Snow Science Workshop, Innsbruck, Austria, pp. 328–332, 2018.

Dall'Amico, M., Tasin, S., Di Paolo, F., Brian, M., Leoni, P., Tornatore, F., Formetta, G., Wani, J. M., Rigon, R., and Roati, G.: 30-years (1991-2021) snow water equivalent dataset in the Po River District, Italy, Sci. Data, 12, 374, https://doi.org/10.1038/s41597-025-04633-5, 2025.

De Lannoy, G. J. M., Bechtold, M., Busschaert, L., Heyvaert, Z., Modanesi, S., Dunmire, D., Lievens, H., Getirana, A., and Massari, C.: Contributions of irrigation modeling, soil moisture and snow data assimilation to high-resolution water budget estimates over the Po basin: Progress towards digital replicas, J. Adv. Model. Earth Syst., 16, e2024MS004 433, https://doi.org/10.1029/2024MS004433, 2024.

Dozier, J.: Mountain hydrology, snow color, and the fourth paradigm, Eos (Washington DC), 92, 373–374, https://doi.org/10.1029/2011EO430001, 2011.

Durand, M., Molotch, N. P., and Margulis, S. A.: A Bayesian approach to snow water equivalent reconstruction, Journal of Geophysical Research: Atmospheres, 113, https://doi.org/10.1029/2008JD009894, 2008.

https://doi.org/10.5194/egusphere-2025-5520
Preprint. Discussion started: 18 December 2025

Edwards, A. C., Scalenghe, R., and Freppaz, M.: Changes in the seasonal snow cover of alpine regions and its effect on soil processes: A review, Quat. Int., 162-163, 172–181, https://doi.org/10.1016/j.quaint.2006.10.027, 2007.

Egli, L., Jonas, T., and Meister, R.: Comparison of different automatic methods for estimating snow water equivalent, Cold Reg. Sci. Technol., 57, 107–115, https://doi.org/10.1016/j.coldregions.2009.02.008, 2009.

Endrizzi, S., Gruber, S., Dall'Amico, M., and Rigon, R.: GEOtop 2.0: simulating the combined energy and water balance at and below the land surface accounting for soil freezing, snow cover and terrain effects, Geosci. Model Dev., 7, 2831–2857, https://doi.org/10.5194/gmd-7-2831-2014, 2014.

Faranda, D., Pascale, S., and Bulut, B.: Persistent anticyclonic conditions and climate change exacerbated the exceptional 2022 European-Mediterranean drought, Environ. Res. Lett., https://doi.org/10.1088/1748-9326/acbc37, 2023.

Formetta, G., Kampf, S. K., David, O., and Rigon, R.: Snow water equivalent modeling components in NewAge-JGrass, Geoscientific Model Development, 7, 725–736, https://doi.org/10.5194/gmd-7-725-2014, 2014.

Gleason, K. E., McConnell, J. R., Arienzo, M. M., Chellman, N., and Calvin, W. M.: Four-fold increase in solar forcing on snow in western U.S. burned forests since 1999, Nat. Commun., 10, 2026, https://doi.org/0.1038/s41467-019-09935-y, 2019.

Gobiet, A., Kotlarski, S., Beniston, M., Heinrich, G., Rajczak, J., and Stoffel, M.: 21st century climate change in the European Alps–a review, Sci. Total Environ., 493, 1138–1151, https://doi.org/10.1016/j.scitotenv.2013.07.050, 2014.

Hersbach, H., Bell, B., Berrisford, P., Hirahara, S., Horányi, A., Muñoz-Sabater, J., Nicolas, J., Peubey, C., Radu, R., Schepers, D., Simmons, A., Soci, C., Abdalla, S., Abellan, X., Balsamo, G., Bechtold, P., Biavati, G., Bidlot, J., Bonavita, M., De Chiara, G., Dahlgren, P., Dee, D., Diamantakis, M., Dragani, R., Flemming, J., Forbes, R., Fuentes, M., Geer, A., Haimberger, L., Healy, S., Hogan, R. J., Hólm, E., Janisková, M., Keeley, S., Laloyaux, P., Lopez, P., Lupu, C., Radnoti, G., de Rosnay, P., Rozum, I., Vamborg, F., Villaume, S., and Jean-Noël Thépaut: The ERA5 global reanalysis, Q. J. R. Meteorol. Soc., 146, 1999–2049, https://doi.org/10.1002/qj.3803, 2020.

Hirsch, R. M., Slack, J. R., and Smith, R. A.: Techniques of trend analysis for monthly water quality data, Water Resources Research, 18, 107–121, https://doi.org/10.1029/WR018i001p00107, 1982.

Hock, R., Rasul, G., Adler, C., Cáceres, B., Gruber, S., Hirabayashi, Y., Jackson, M., Kääb, A., Kang, S., Kutuzov, S., Milner, A., Molau, U., Morin, S., Orlove, B., and Steltzer, H.: High mountain areas, in: IPCC Special Report on the Ocean and Cryosphere in a Changing Climate, edited by H.-O. Pörtner, D.C. Roberts, V. Masson-Delmotte, P. Zhai, M. Tignor, E. Poloczanska, K. Mintenbeck, A. Alegría, M. Nicolai, A. Okem, J. Petzold, B. Rama, N.M. Weyer, pp. 131–202, Cambridge University Press, https://doi.org/10.1017/9781009157964.004, 2019.

Huning, L. S. and AghaKouchak, A.: Global snow drought hot spots and characteristics, Proc. Natl. Acad. Sci. U. S. A., 117, 19 753–19 759, https://doi.org/10.1073/pnas.1915921117, 2020.

Huss, M., Bookhagen, B., Huggel, C., Jacobsen, D., Bradley, R. S., Clague, J. J., Vuille, M., Buytaert, W., Cayan, D. R., Greenwood, G., Mark, B. G., Milner, A. M., Weingartner, R., and Winder, M.: Toward mountains without permanent snow and ice, Earths Future, 5, 418–435, https://doi.org/10.1002/2016EF000514, 2017.

IPCC: Sections, in: Climate Change 2023: Synthesis Report. Contribution of Working Groups I, II and III to the Sixth Assessment Report of the Intergovernmental Panel on Climate Change, edited by Core Writing Team, H. Lee and J. Romero (eds.)], pp. 35–115, IPCC, Geneva, Switzerland, https://doi.org/10.59327/IPCC/AR6-9789291691647, 2023.

J. G. Arnold, D. N. Moriasi, P. W. Gassman, K. C. Abbaspour, M. J. White, R. Srinivasan, C. Santhi, R. D. Harmel, A. van Griensven, M. W. Van Liew, N. Kannan, and M. K. Jha: SWAT: Model use, calibration, and validation, Trans. ASABE, 55, 1491–1508, https://doi.org/10.13031/2013.42256, 2012.

https://doi.org/10.5194/egusphere-2025-5520
Preprint. Discussion started: 18 December 2025

Jenicek, M., Seibert, J., and Staudinger, M.: Modeling of Future Changes in Seasonal Snowpack and Impacts on Summer Low Flows in Alpine Catchments, Water Resources Research, 54, 538–556, https://doi.org/10.1002/2017WR021648, 2018.

Jiao, D., Xu, N., Yang, F., and Xu, K.: Evaluation of spatial-temporal variation performance of ERA5 precipitation data in China, Sci. Rep., 11, 17 956, https://doi.org/10.1038/s41598-021-97432-y, 2021.

Kendall, M. G.: Rank Correlation Methods, 1962.

Koehler, J., Dietz, A. J., Zellner, P., Baumhoer, C. A., Dirscherl, M., Cattani, L., Vlahovic, Z., Alasawedah, M. H., Mayer, K., Haslinger, K., Bertoldi, G., Jacob, A., and Kuenzer, C.: Drought in Northern Italy: Long earth observation time series reveal snow line elevation to be several hundred meters above long-term average in 2022, Remote Sens. (Basel), 14, 6091, https://doi.org/10.3390/rs14236091, 2022.

Kotlarski, S., Gobiet, A., Morin, S., Olefs, M., Rajczak, J., and Samacoïts, R.: 21st Century alpine climate change, Clim. Dyn., 60, 65–86, https://doi.org/10.1007/s00382-022-06303-3, 2022.

Kwon, Y., Yoon, Y., Forman, B. A., Kumar, S. V., and Wang, L.: Quantifying the observational requirements of a space-borne LiDAR snow mission, J. Hydrol. (Amst.), 601, 126 709, https://doi.org/10.1016/j.jhydrol.2021.126709, 2021.

Lawrimore, J. H., Menne, M. J., Gleason, B. E., Williams, C. N., Wuertz, D. B., Vose, R. S., and Rennie, J.: An overview of the Global Historical Climatology Network monthly mean temperature data set, version 3, Journal of Geophysical Research: Atmospheres, 116, https://doi.org/10.1029/2011JD016187, 2011.

LIFE CLIMAX PO Project: Il Progetto, https://www.lifeclimaxpo.adbpo.it/il-progetto/, 2023.

Ma, X., Li, D., Fang, Y., Margulis, S. A., and Lettenmaier, D. P.: Estimating spatiotemporally continuous snow water equivalent from intermittent satellite observations: an evaluation using synthetic data, Hydrol. Earth Syst. Sci., 27, 21–38, https://doi.org/10.5194/hess-27-21-2023, 2023.

Mann, H. B.: Nonparametric Tests Against Trend, Econometrica, 13, 245, https://doi.org/0.2307/1907187, 1945.

Marcolini, G., Bellin, A., Disse, M., and Chiogna, G.: Variability in snow depth time series in the Adige catchment, J. Hydrol. Reg. Stud., 13, 240–254, https://doi.org/10.1016/j.ejrh.2017.08.007, 2017.

Margulis, S. A., Girotto, M., Cortés, G., and Durand, M.: A Particle Batch Smoother Approach to Snow Water Equivalent Estimation, J. Hydrometeorol., 16, 1752–1772, https://doi.org/10.1175/JHM-D-14-0177.1, 2015.

Margulis, S. A., Fang, Y., Li, D., Lettenmaier, D. P., and Andreadis, K.: The utility of infrequent snow depth images for deriving continuous space-time estimates of seasonal snow water equivalent, Geophys. Res. Lett., 46, 5331–5340, https://doi.org/10.1175/JHM-D-14-0177.1, 2019.

Marty, C.: Regime shift of snow days in Switzerland, Geophys. Res. Lett., 35, https://doi.org/10.1029/2008GL033998, 2008.

Marty, C., Rohrer, M. B., Huss, M., and Stähli, M.: Multi-decadal observations in the alps reveal less and wetter snow, with increasing variability, Front. Earth Sci., 11, 1165 861, https://doi.org/10.3389/feart.2023.1165861, 2023.

Matiu, M., Crespi, A., Bertoldi, G., Carmagnola, C. M., Marty, C., Morin, S., Schöner, W., Cat Berro, D., Chiogna, G., De Gregorio, L., Kotlarski, S., Majone, B., Resch, G., Terzago, S., Valt, M., Beozzo, W., Cianfarra, P., Gouttevin, I., Marcolini, G., Notarnicola, C., Petitta, M., Scherrer, S. C., Strasser, U., Winkler, M., Zebisch, M., Cicogna, A., Cremonini, R., Debernardi, A., Faletto, M., Gaddo, M., Giovannini, L., Mercalli, L., Soubeyroux, J.-M., Sušnik, A., Trenti, A., Urbani, S., and Weilguni, V.: Observed snow depth trends in the European Alps: 1971 to 2019, Cryosphere, 15, 1343–1382, https://doi.org/10.5194/tc-15-1343-2021, 2021.

Molotch, N. P.: Reconstructing snow water equivalent in the Rio Grande headwaters using remotely sensed snow cover data and a spatially distributed snowmelt model, Hydrol. Process., 23, 1076–1089, https://doi.org/10.1002/hyp.7206, 2009.

https://doi.org/10.5194/egusphere-2025-5520
Preprint. Discussion started: 18 December 2025

Molotch, N. P. and Bales, R. C.: SNOTEL representativeness in the Rio Grande headwaters on the basis of physiographics and remotely sensed snow cover persistence, Hydrol. Process., 20, 723–739, https://doi.org/10.1002/hyp.6128, 2006.

Montanari, A., Nguyen, H., Rubinetti, S., Ceola, S., Galelli, S., Rubino, A., and Zanchettin, D.: Why the 2022 Po River drought is the worst in the past two centuries, Sci Adv, 9, eadg8304, https://doi.org/10.1126/sciadv.adg8304, 2023.

Monteiro, D. and Morin, S.: Multi-decadal analysis of past winter temperature, precipitation and snow cover data in the European Alps from reanalyses, climate models and observational datasets, Cryosphere, 17, 3617–3660, https://doi.org/10.5194/tc-17-3617-2023, 2023.

Mote, P., Hamlet, A., and Salathe, E.: Has spring snowpack declined in the Washington Cascades?, Hydrol. Earth Syst. Sci., 12, 193–206, https://doi.org/10.5194/hess-12-193-2008, 2008.

Mote, P. W.: Climate-driven variability and trends in mountain snowpack in western North America, J. Clim., 19, 6209–6220, https://doi.org/10.1175/JCLI3971.1, 2006.

Mote, P. W., Li, S., Lettenmaier, D. P., Xiao, M., and Engel, R.: Dramatic declines in snowpack in the western US, Npj Clim. Atmos. Sci., 1, 1–6, https://doi.org/10.1038/s41612-018-0012-1, 2018.

Mountain Research Initiative EDW Working Group: Elevation-dependent warming in mountain regions of the world, Nat. Clim. Chang., 5, 424–430, https://doi.org/10.1038/nclimate2563, 2015.

Muñoz-Sabater, J., Dutra, E., Agustí-Panareda, A., Albergel, C., Arduini, G., Balsamo, G., Boussetta, S., Choulga, M., Harrigan, S., Hersbach, H., Martens, B., Miralles, D. G., Piles, M., Rodríguez-Fernández, N. J., Zsoter, E., Buontempo, C., and Jean-Noël Thépaut: ERA5-Land: a state-of-the-art global reanalysis dataset for land applications, Earth Syst. Sci. Data, 13, 4349–4383, https://doi.org/10.5194/essd-13-4349-2021, 2021.

Notarnicola, C.: Hotspots of snow cover changes in global mountain regions over 2000–2018, Remote Sens. Environ., 243, 111 781, https://doi.org/10.1016/j.rse.2020.111781, 2020.

Notarnicola, C.: Overall negative trends for snow cover extent and duration in global mountain regions over 1982-2020, Sci. Rep., 12, 13 731, https://doi.org/10.1038/s41598-022-16743-w, 2022.

Oveisgharan, S., Zinke, R., Hoppinen, Z., and Marshall, H. P.: Snow water equivalent retrieval over Idaho – Part 1: Using Sentinel-1 repeat-pass interferometry, Cryosphere, 18, 559–574, https://doi.org/10.5194/tc-18-559-2024, 2024.

Pederson, G. T., Gray, S. T., Woodhouse, C. A., Betancourt, J. L., Fagre, D. B., Littell, J. S., Watson, E., Luckman, B. H., and Graumlich, L. J.: The unusual nature of recent snowpack declines in the North American cordillera, Science, 333, 332–335, https://doi.org/10.1126/science.1201570, 2011.

Premier, V., Marin, C., Bertoldi, G., Barella, R., Notarnicola, C., and Bruzzone, L.: Exploring the use of multi-source high-resolution satellite data for snow water equivalent reconstruction over mountainous catchments, The Cryosphere, 17, 2387–2407, https://doi.org/10.5194/tc-17-2387-2023, 2023.

Schattan, P., Köhli, M., Schrön, M., Baroni, G., and Oswald, S. E.: Sensing area-average snow water equivalent with cosmic-ray neutrons: The influence of fractional snow cover, Water Resour. Res., 55, 10 796–10 812, https://doi.org/10.1029/2019WR025647, 2019.

Schilling, S., Dietz, A., and Kuenzer, C.: Snow water equivalent monitoring—A review of large-scale remote sensing applications, Remote Sens. (Basel), 16, 1085, https://doi.org/10.3390/rs16061085, 2024.

Serreze, M. C., Clark, M. P., and Frei, A.: Characteristics of large snowfall events in the montane western United States as examined using snowpack telemetry (SNOTEL) data, Water Resour. Res., 37, 675–688, https://doi.org/10.1029/2000WR900307, 2001.

https://doi.org/10.5194/egusphere-2025-5520
Preprint. Discussion started: 18 December 2025

Shahgedanova, M., Adler, C., Gebrekirstos, A., Grau, H. R., Huggel, C., Marchant, R., Pepin, N., Vanacker, V., Viviroli, D., and Vuille, M.: Mountain observatories: Status and prospects for enhancing and connecting a global community, Mt. Res. Dev., 41, A1, https://doi.org/10.1659/MRD-JOURNAL-D-20-00054.1, 2021.

Shrestha, S., Zaramella, M., Callegari, M., Greifeneder, F., and Borga, M.: Scale dependence of errors in snow water equivalent simulations using ERA5 reanalysis over alpine basins, Climate, 11, 154, https://doi.org/10.3390/cli11070154, 2023.

Smoot, E. E. and Gleason, K. E.: Forest fires reduce snow-water storage and advance the timing of snowmelt across the western U.s, Water (Basel), 13, 3533, https://doi.org/10.3390/w13243533, 2021.

Sommer, C., Malz, P., Seehaus, T. C., Lippl, S., Zemp, M., and Braun, M. H.: Rapid glacier retreat and downwasting throughout the European Alps in the early 21st century, Nat. Commun., 11, 3209, https://doi.org/10.1038/s41467-020-16818-0, 2020.

Stewart, I. T.: Changes in snowpack and snowmelt runoff for key mountain regions, Hydrol. Process., 23, 78–94, https://doi.org/10.1002/hyp.7128, 2009.

Stone, R. S., Dutton, E. G., Harris, J. M., and Longenecker, D.: Earlier spring snowmelt in northern Alaska as an indicator of climate change, Journal of Geophysical Research: Atmospheres, 107, ACL 10–1–ACL 10–13, https://doi.org/10.1029/2000JD000286, 2002.

Sturm, M., Taras, B., Liston, G. E., Derksen, C., Jonas, T., and Lea, J.: Estimating snow water equivalent using snow depth data and climate classes, J. Hydrometeorol., 11, 1380–1394, https://doi.org/10.1175/2010JHM1202.1, 2010.

Tsang, L., Durand, M., Derksen, C., Barros, A. P., Kang, D.-H., Lievens, H., Marshall, H.-P., Zhu, J., Johnson, J., King, J., Lemmetyinen, J., Sandells, M., Rutter, N., Siqueira, P., Nolin, A., Osmanoglu, B., Vuyovich, C., Kim, E., Taylor, D., Merkouriadi, I., Brucker, L., Navari, M., Dumont, M., Kelly, R., Kim, R. S., Liao, T.-H., Borah, F., and Xu, X.: Review article: Global monitoring of snow water equivalent using high-frequency radar remote sensing, Cryosphere, 16, 3531–3573, https://doi.org/10.5194/tc-16-3531-2022, 2022.

Viviroli, D., Dürr, H. H., Messerli, B., Meybeck, M., and Weingartner, R.: Mountains of the world, water towers for humanity: Typology, mapping, and global significance, Water Resour. Res., 43, https://doi.org/10.1029/2006WR005653, 2007.

Viviroli, D., Archer, D. R., Buytaert, W., Fowler, H. J., Greenwood, G. B., Hamlet, A. F., Huang, Y., Koboltschnig, G., Litaor, M. I., López-Moreno, J. I., Lorentz, S., Schädler, B., Schreier, H., Schwaiger, K., Vuille, M., and Woods, R.: Climate change and mountain water resources: overview and recommendations for research, management and policy, Hydrol. Earth Syst. Sci., 15, 471–504, https://doi.org/10.5194/hess-15-471-2011, 2011.

Yue, S., Pilon, P., Phinney, B., and Cavadias, G.: The influence of autocorrelation on the ability to detect trend in hydrological series, Hydrol. Process., 16, 1807–1829, https://doi.org/10.1002/hyp.1095, 2002.

Zampieri, M., Scoccimarro, E., Gualdi, S., and Navarra, A.: Observed shift towards earlier spring discharge in the main Alpine rivers, Sci. Total Environ., 503-504, 222–232, https://doi.org/10.1016/j.scitotenv.2014.06.036, 2015.

https://doi.org/10.5194/egusphere-2025-5520
Preprint. Discussion started: 18 December 2025

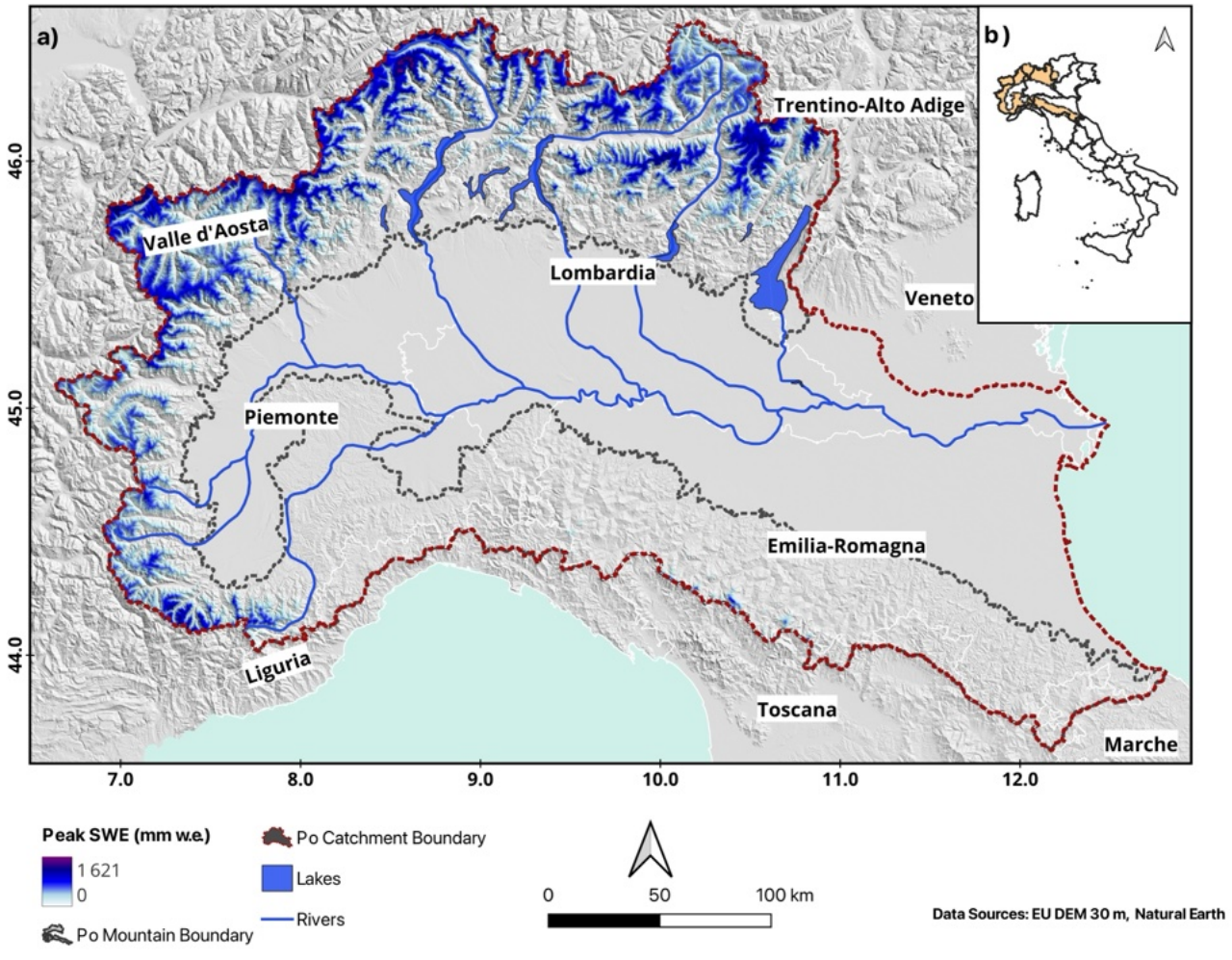

Figure 1. a) Overview map of the Po River District (red and dashed) showing the topographic and hydrological features annotated with region names. Blue colored overlay shows the long-term peak SWE distribution for the period 1991-2021. The study domain, i.e., the mountain part of the Po River District is shown in black and dashed boundary, b) Location of the study domain within the map of Italy, highlighted in yellow color.

https://doi.org/10.5194/egusphere-2025-5520
Preprint. Discussion started: 18 December 2025

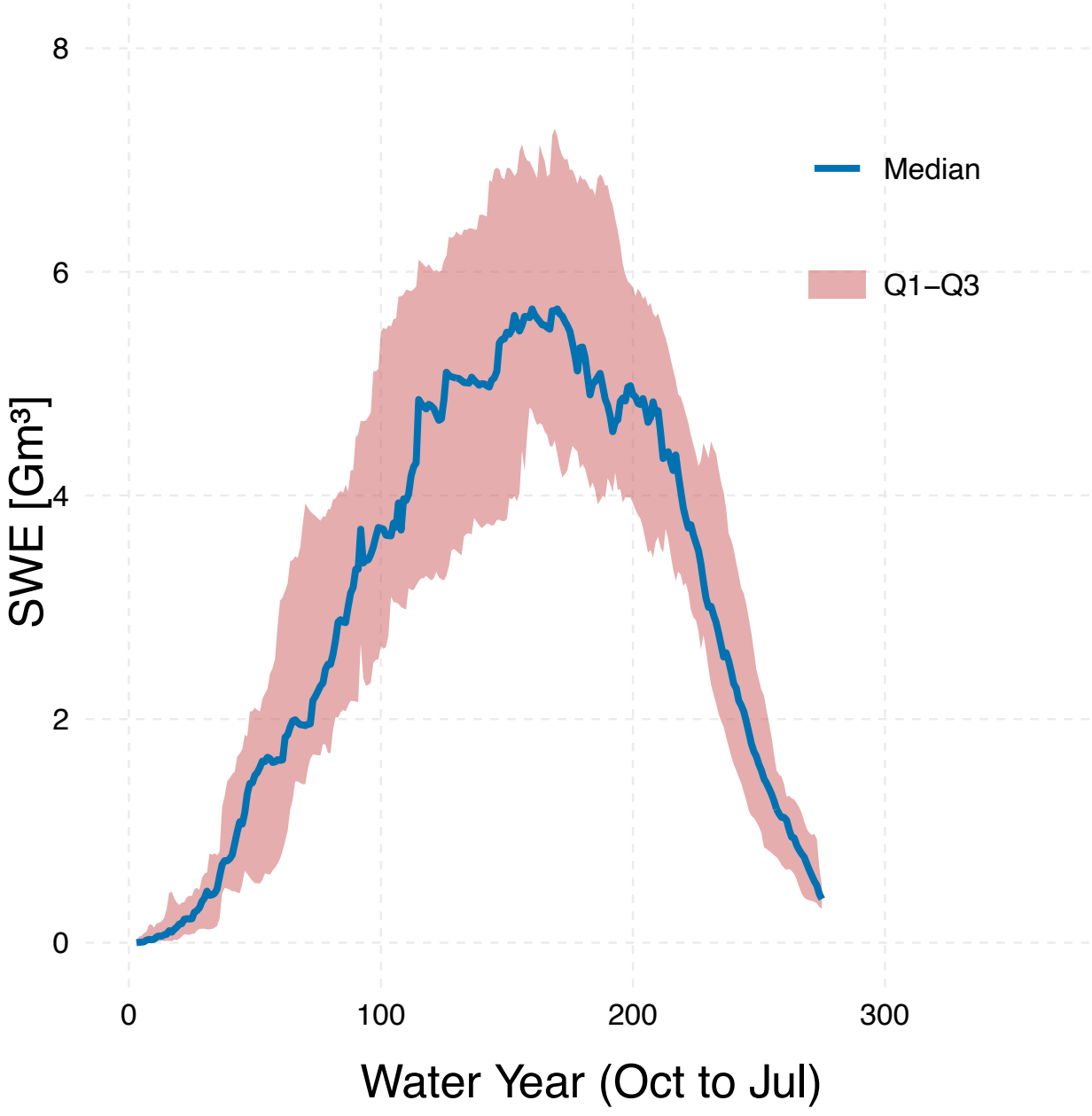

Figure 2. Annual cycle of the basin-wide SWE volume (Gm^3) for the 30-year period (1991-2021). The red ribbon shows the inter-quartile range (Q1-Q3) for the reference period, whereas the blue line represents the median.

https://doi.org/10.5194/egusphere-2025-5520
Preprint. Discussion started: 18 December 2025

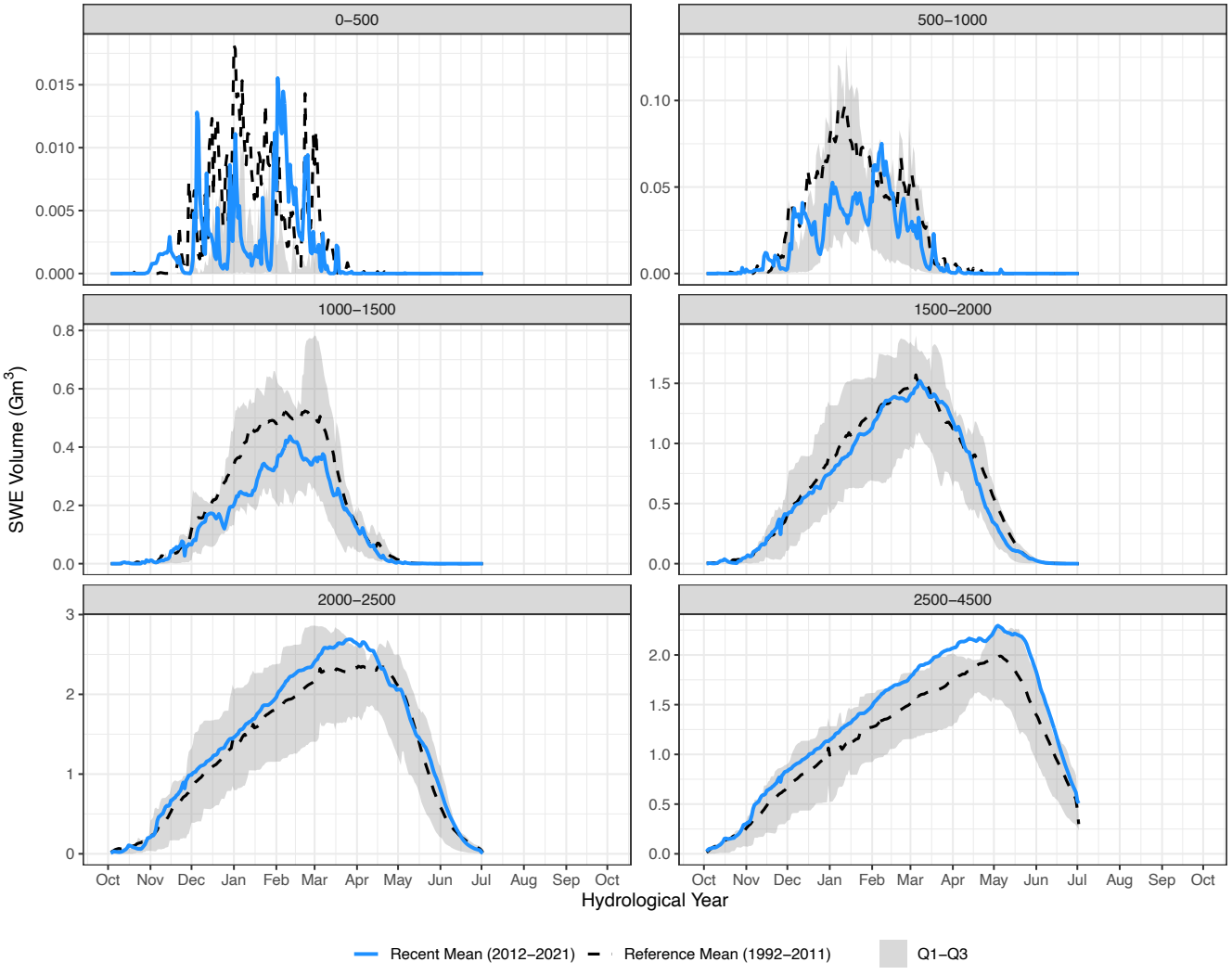

Figure 3. Comparison of basin-wide volume of water (Gm^3) in different elevation bands. It highlights the mean daily SWE for the period 2012-2021 (blue line) against the 1992-2011 baseline (black dashed). The gray ribbon shows the inter-quartile range (Q1-Q3) for the reference period.

https://doi.org/10.5194/egusphere-2025-5520
Preprint. Discussion started: 18 December 2025

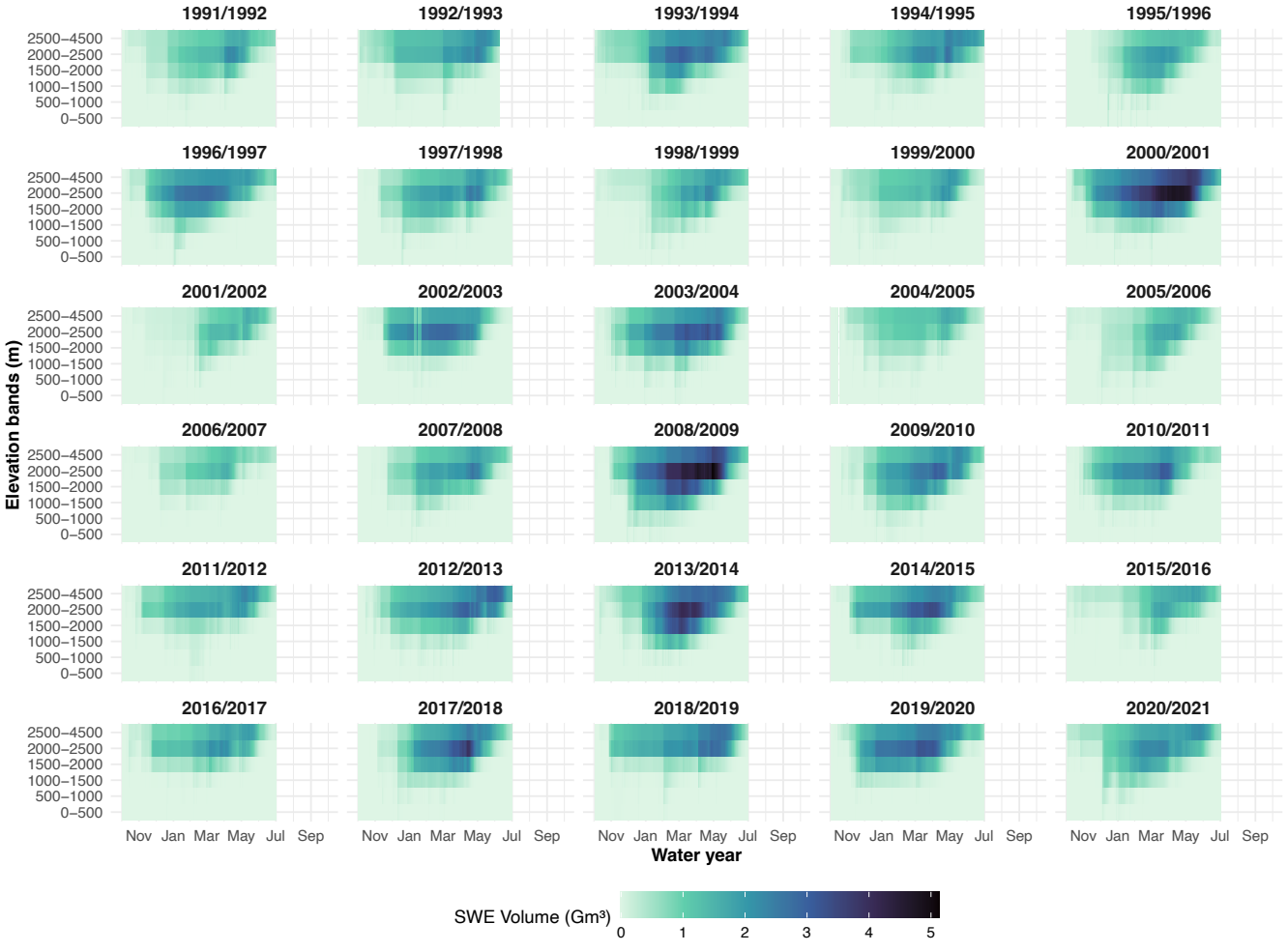

Figure 4. Spatiotemporal evolution of seasonal snowpack across the study domain using Hovmöller plot of daily elevation-wise volume of water from SWE in each water year from 1991/1992 to 2020/2021.

https://doi.org/10.5194/egusphere-2025-5520
Preprint. Discussion started: 18 December 2025

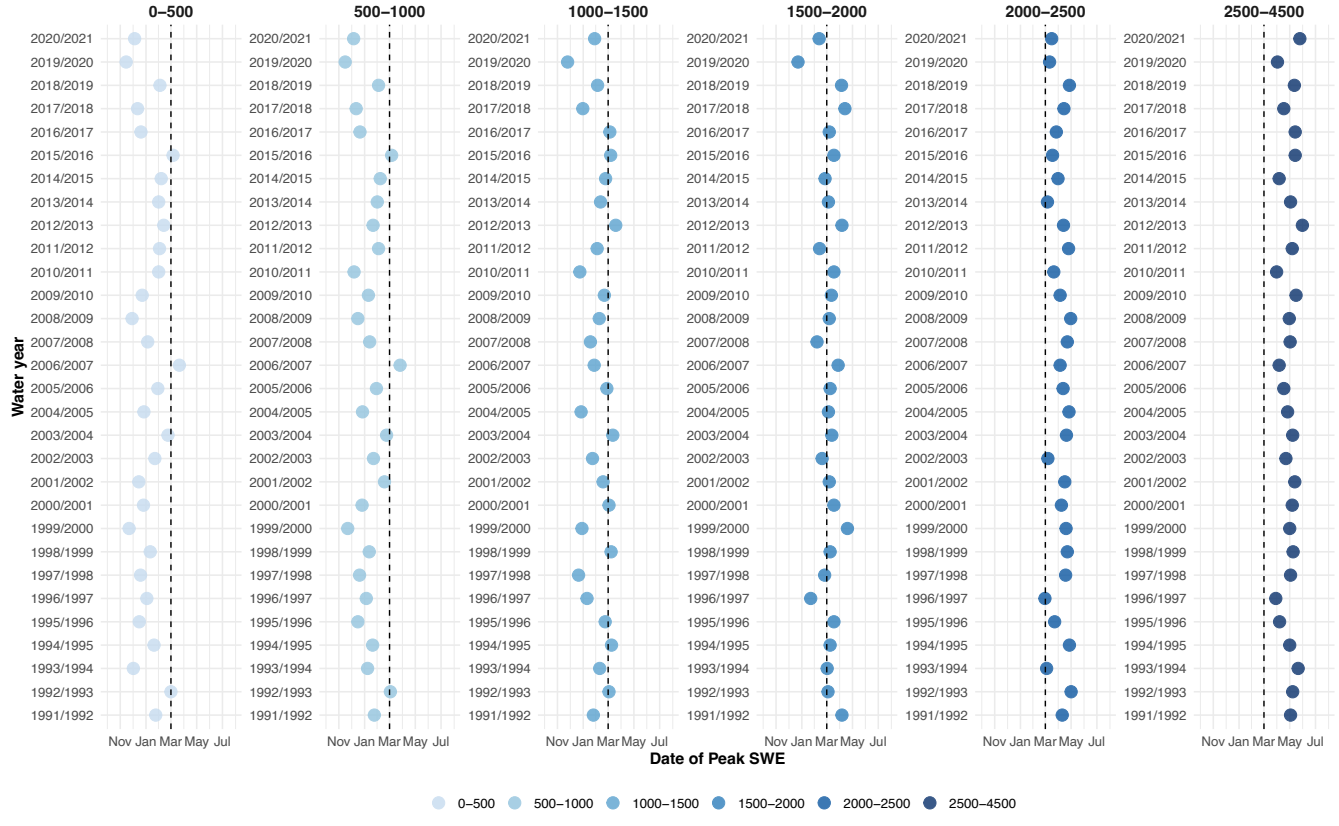

Figure 5. Elevation-wise timing of peak snow water equivalent occurrence during the period 1991–2021 in the Po River Basin, Italy with dashed vertical line indicating conventional peak SWE in Italy, i.e., March 6 (Avanzi et al., 2024).

https://doi.org/10.5194/egusphere-2025-5520
Preprint. Discussion started: 18 December 2025

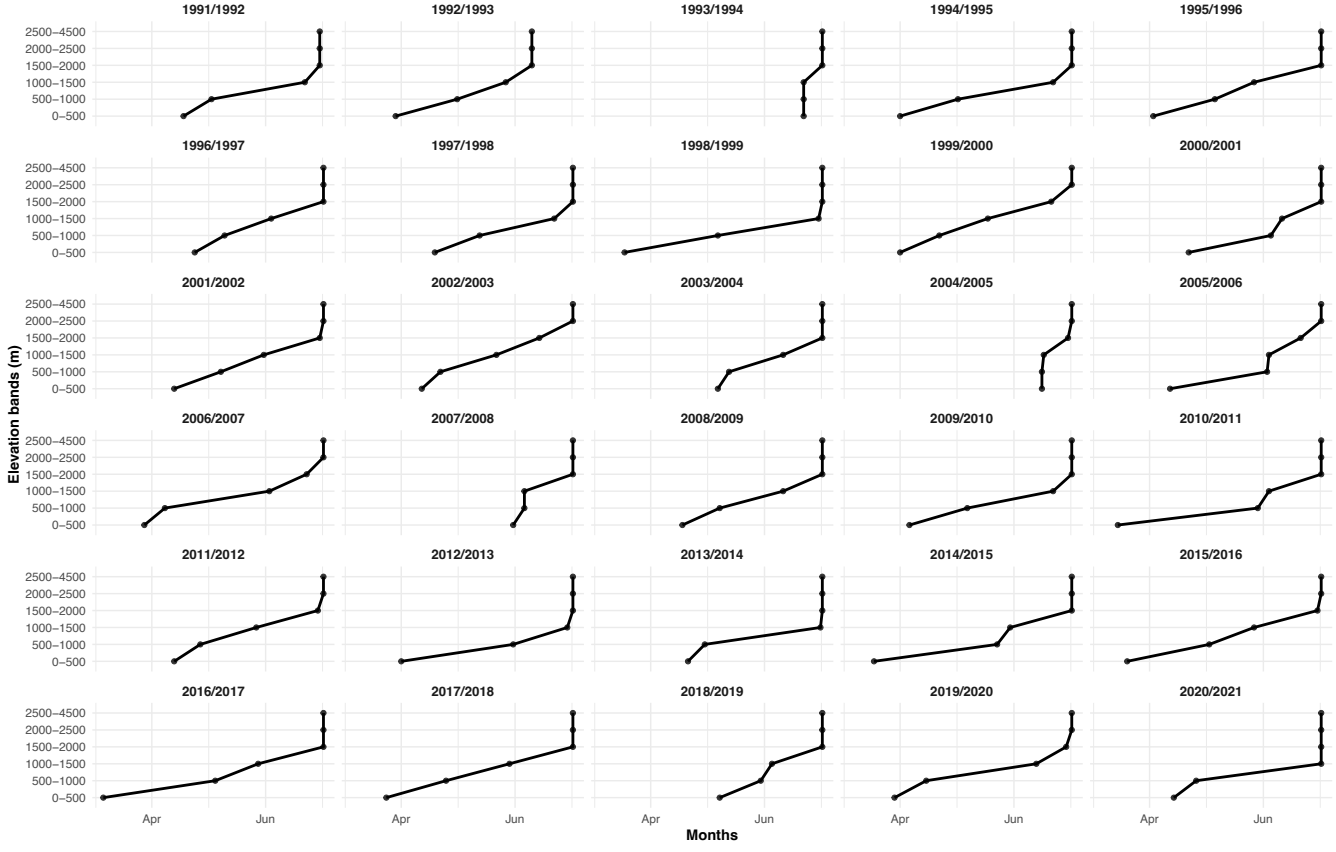

Figure 6. Elevation-wise snow disappearance date during the period 1991–2021 in the Po River Basin, Italy. Each subplot represents a single water year.

https://doi.org/10.5194/egusphere-2025-5520
Preprint. Discussion started: 18 December 2025

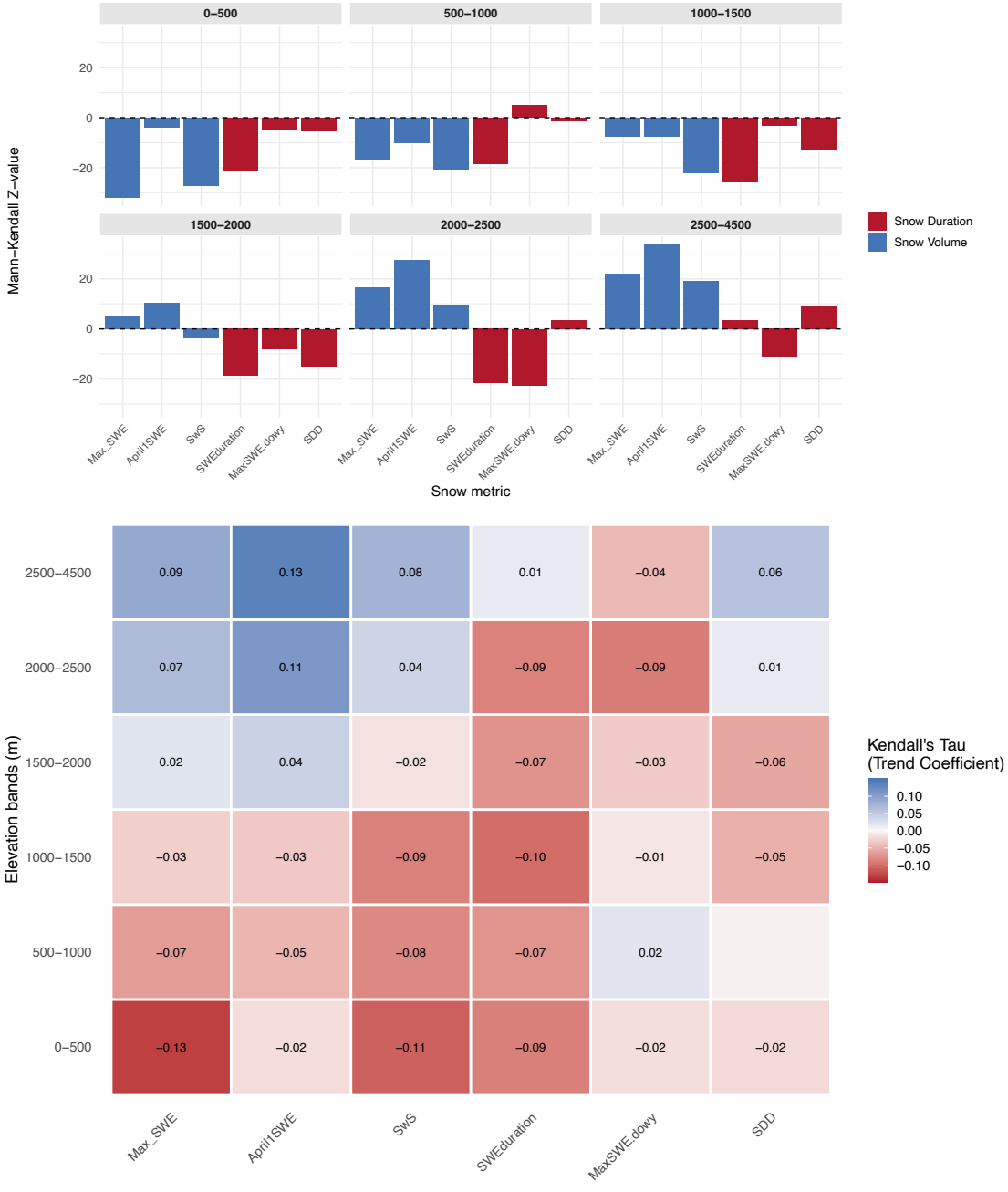

Figure 7. Statistical analysis of six key snow metrics across different elevation bands.

https://doi.org/10.5194/egusphere-2025-5520
Preprint. Discussion started: 18 December 2025

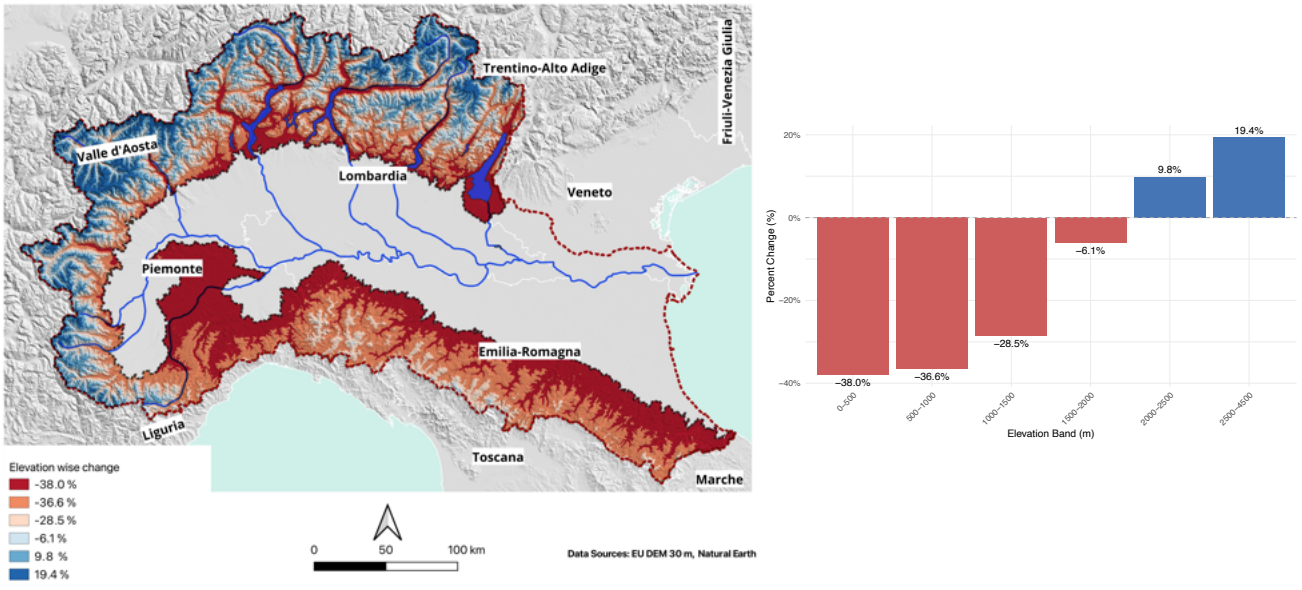

Figure 8. Percentage change in total volume of water (Elevation-wise) for the period 1991 to 2021. It highlights the change in the recent decade with reference to mean of first two decades. The relative percentage change was calculated: Overall_Percentage_Change = New_Value (2012-2021)- Old_Value (1991-2011) / Old_Value (1991-2011) × 100.

https://doi.org/10.5194/egusphere-2025-5520
Preprint. Discussion started: 18 December 2025

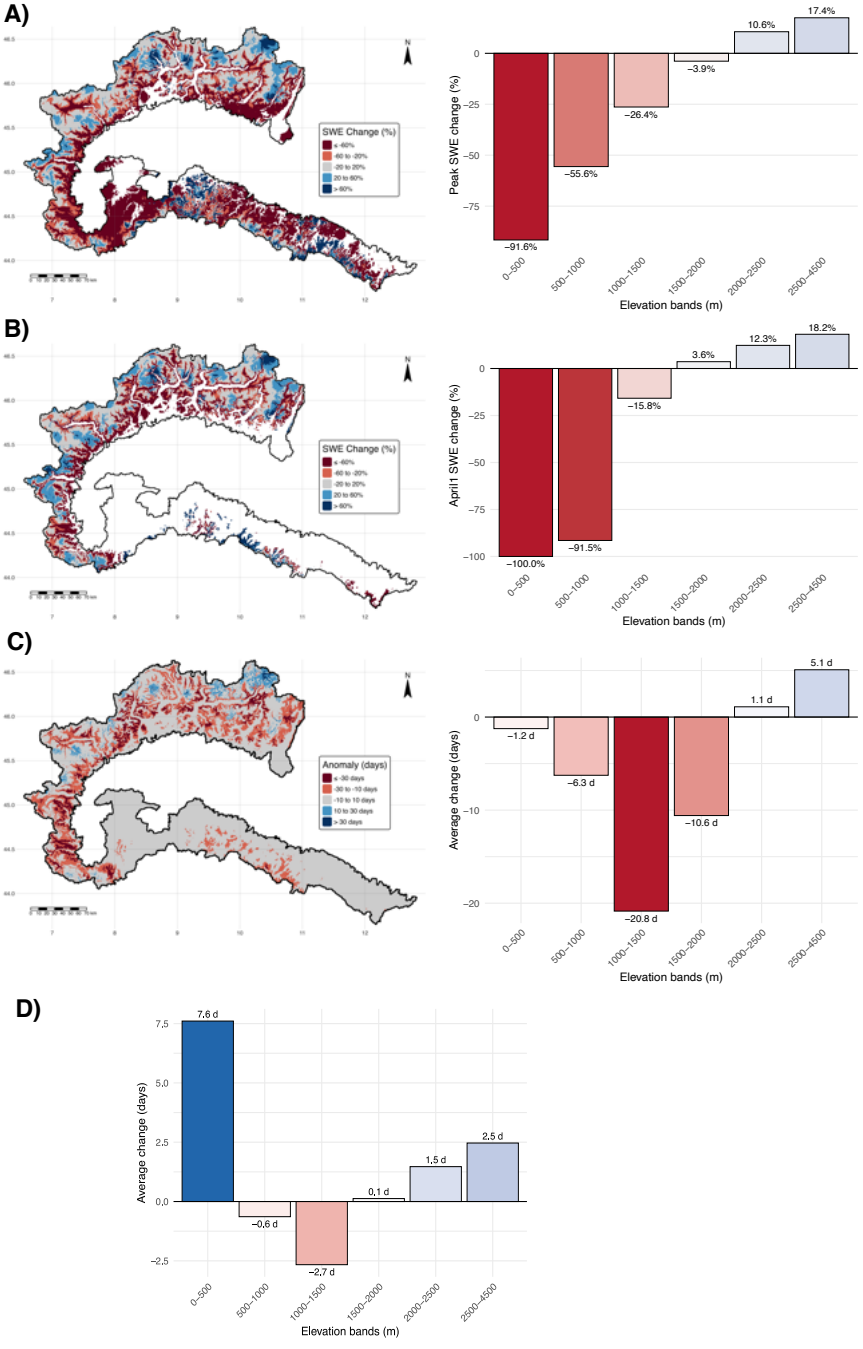

Figure 9. Elevation-wise anomalies of SWE magnitude: (A) Peak SWE and (B) April 1 SWE, and (C) snow duration, and (D) snow disappearance dates across different elevation bands between the recent decade (2012-2021) and the reference decades (1992-2011).

https://doi.org/10.5194/egusphere-2025-5520
Preprint. Discussion started: 18 December 2025

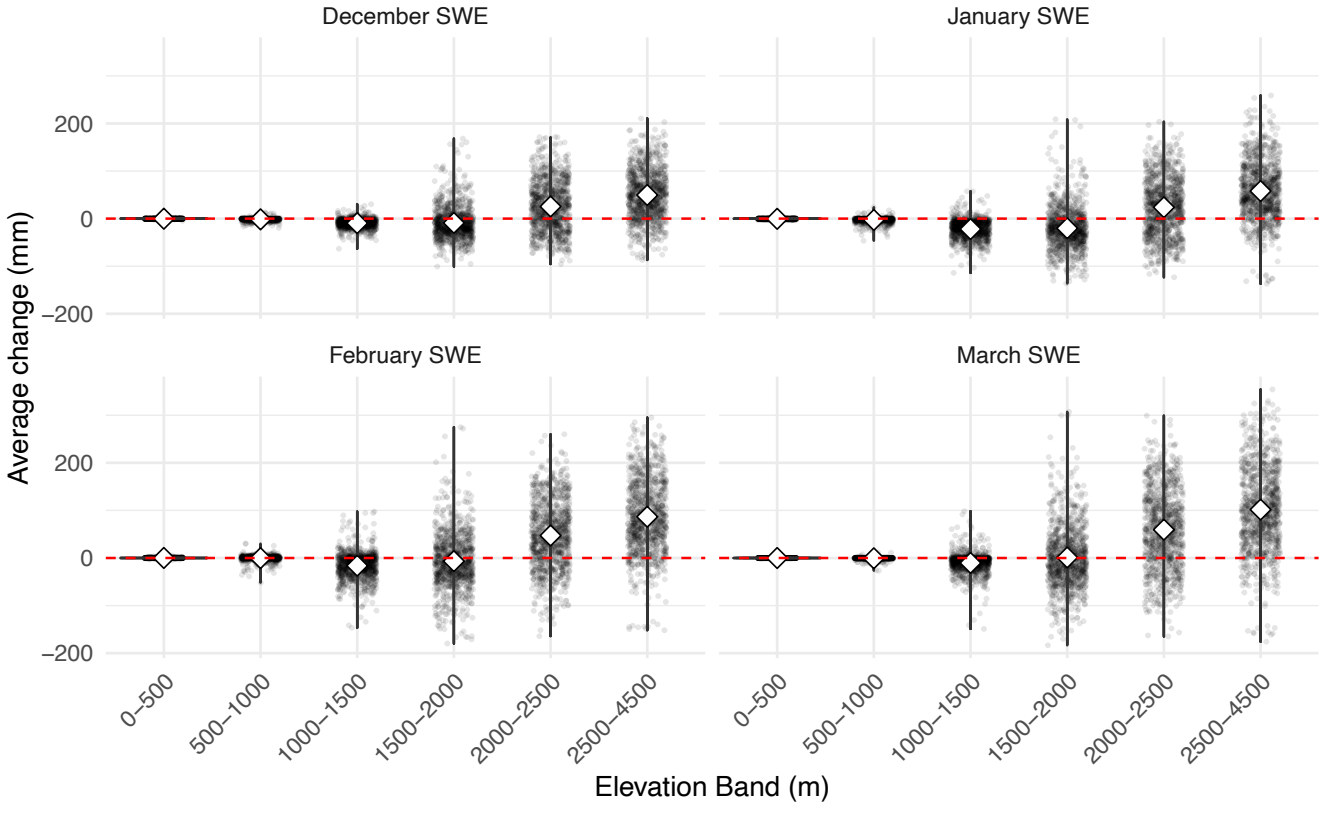

Figure 10. Elevation-wise SWE anomalies across different elevation bands for winter months (December, January, February and March) between the recent decade (2012-2021) and the reference decades (1992-2011).

https://doi.org/10.5194/egusphere-2025-5520
Preprint. Discussion started: 18 December 2025

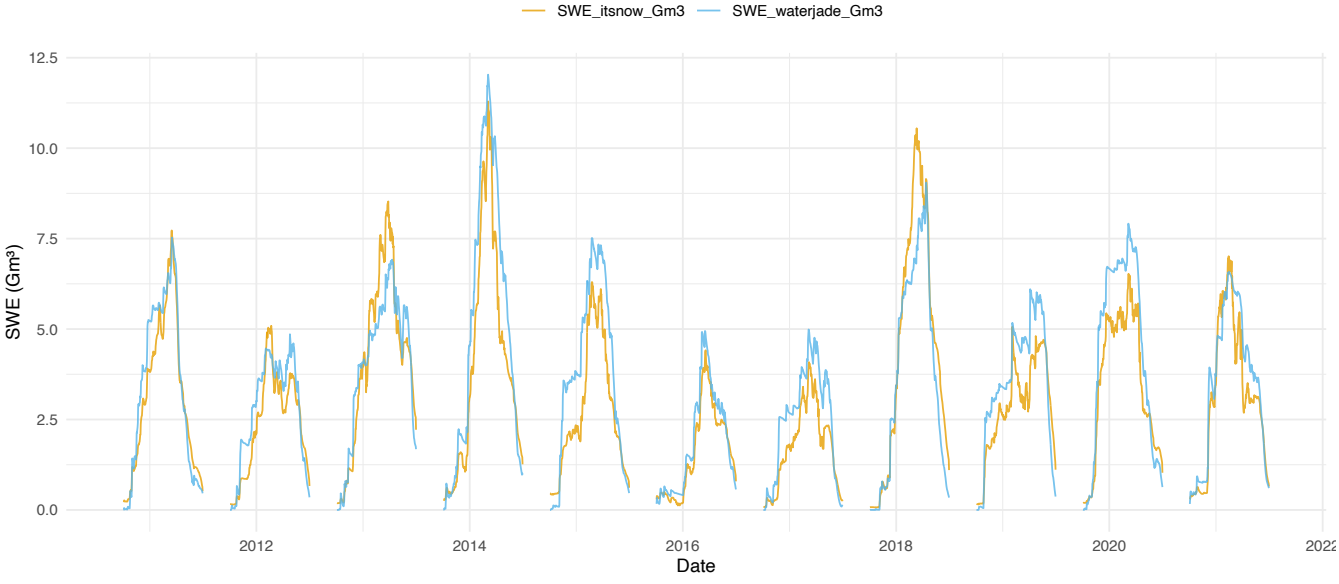

Figure 11. Comparison of daily basin–wide snow volume from the IT-SNOW dataset and WaterJade dataset for the period 2011–2021.

https://doi.org/10.5194/egusphere-2025-5520
Preprint. Discussion started: 18 December 2025

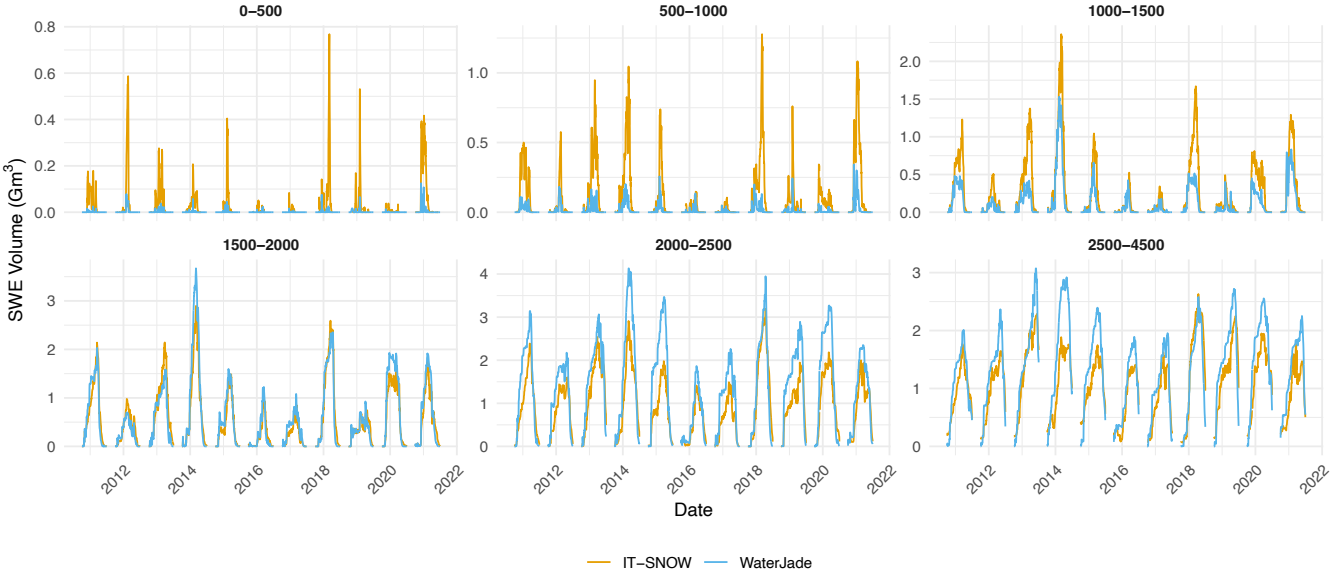

Figure 12. Comparison of daily basin–wide snow volume in different elevation bands from the IT-SNOW dataset and WaterJade dataset for the period 2011–2021.

https://doi.org/10.5194/egusphere-2025-5520
Preprint. Discussion started: 18 December 2025

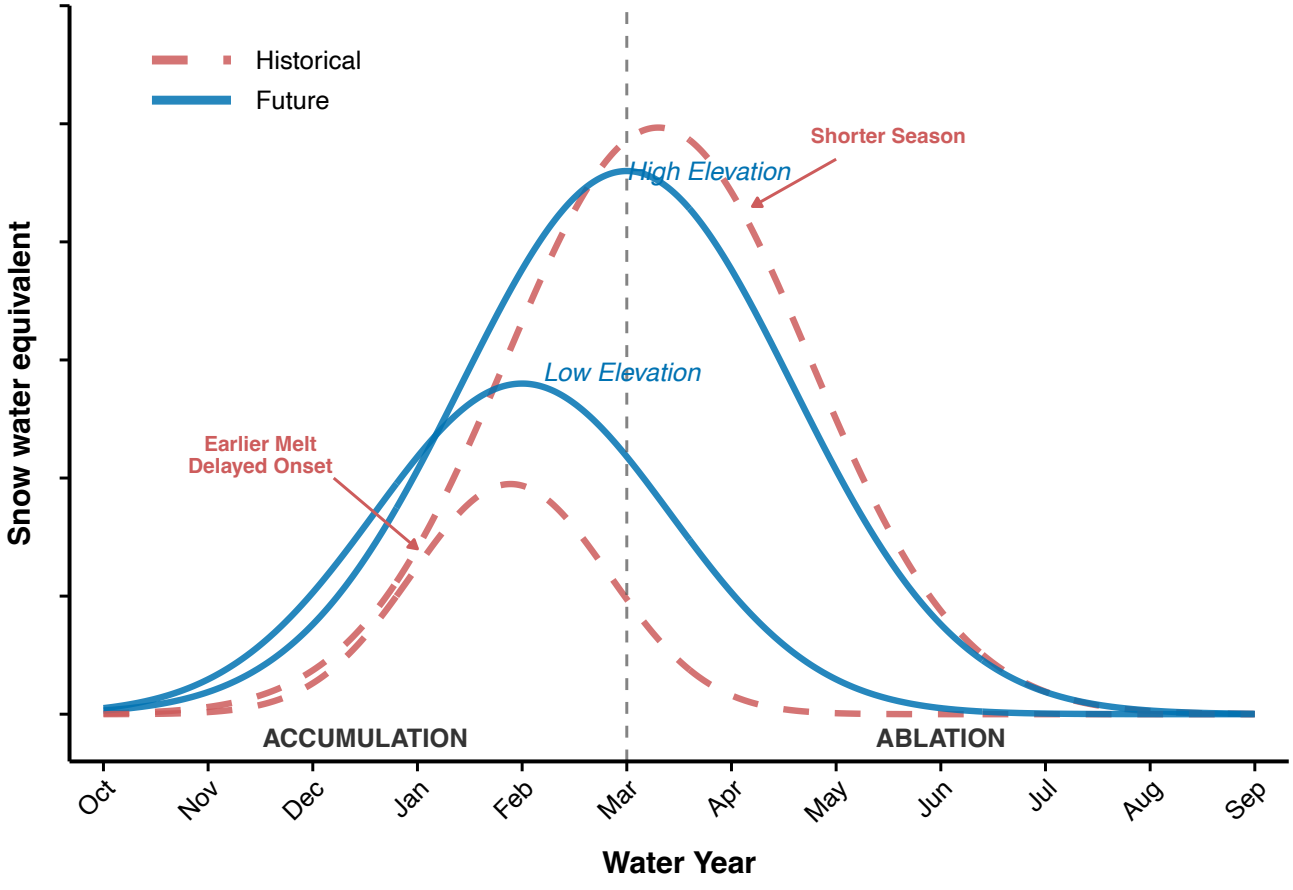

Figure 13. Hypothesis sketch of niveograph highlighting the future changes in SWE due to global warming.

https://doi.org/10.5194/egusphere-2025-5520
Preprint. Discussion started: 18 December 2025

Table 1. Decadal basin-wide SWE volume (Gm^3) by elevation band

Decade	0-500 m	500-1000 m	1000-1500 m	1500-2000 m	2000-2500 m	2500-4500 m	Total
1992-2001	6.5	49.4	449.2	1659.4	3605.5	3364.2	9134.2
2002-2011	8.4	72.6	514.8	1795.1	3349.1	2798.0	8538.0
2012-2021	4.6	38.6	344.7	1622.3	3817.8	3679.4	9507.4

https://doi.org/10.5194/egusphere-2025-5520
Preprint. Discussion started: 18 December 2025

Table 2. Statistical analysis of six key snow metrics across different elevation bands.

ID	Elevation (m)	Stats	Z	Tau (τ)	P-value (p)	Significance
1	0-500	Max SWE	-32.00	-0.13	1.19E-224	Significant
2	0-500	April1SWE	-3.86	-0.02	1.12E-04	Significant
3	0-500	SwS	-27.01	-0.11	1.24E-160	Significant
4	0-500	SWEduration	-21.02	-0.09	4.48E-98	Significant
5	0-500	MaxSWE.dowy	-4.49	-0.02	7.20E-06	Significant
6	0-500	SDD	-5.33	-0.02	9.67E-08	Significant
7	500-1000	Max SWE	-16.76	-0.07	4.64E-63	Significant
8	500-1000	April1SWE	-10.13	-0.05	3.91E-24	Significant
9	500-1000	SwS	-20.49	-0.08	2.53E-93	Significant
10	500-1000	SWEduration	-18.31	-0.07	6.51E-75	Significant
11	500-1000	MaxSWE.dowy	4.83	0.02	1.35E-06	Significant
12	500-1000	SDD	-1.18	-0.00	2.37E-01	NOT Significant
13	1000-1500	Max SWE	-7.30	-0.03	2.96E-13	Significant
14	1000-1500	April1SWE	-7.56	-0.03	3.89E-14	Significant
15	1000-1500	SwS	-22.09	-0.09	3.63E-108	Significant
16	1000-1500	SWEduration	-25.60	-0.10	1.60E-144	Significant
17	1000-1500	MaxSWE.dowy	-3.27	-0.01	1.06E-03	Significant
18	1000-1500	SDD	-13.09	-0.05	3.63E-39	Significant
19	1500-2000	Max SWE	5.09	0.02	3.59E-07	Significant
20	1500-2000	April1SWE	10.36	0.04	3.93E-25	Significant
21	1500-2000	SwS	-3.86	-0.02	1.15E-04	Significant
22	1500-2000	SWEduration	-18.75	-0.07	1.92E-78	Significant
23	1500-2000	MaxSWE.dowy	-8.08	-0.03	6.48E-16	Significant
24	1500-2000	SDD	-14.85	-0.06	6.75E-50	Significant
25	2000-2500	Max SWE	16.66	0.07	2.71E-62	Significant
26	2000-2500	April1SWE	27.41	0.11	2.29E-165	Significant
27	2000-2500	SwS	9.82	0.04	9.50E-23	Significant
28	2000-2500	SWEduration	-21.73	-0.09	1.13E-104	Significant
29	2000-2500	MaxSWE.dowy	-22.52	-0.09	2.91E-112	Significant
30	2000-2500	SDD	3.36	0.01	7.80E-04	Significant
31	2500-4500	Max SWE	22.07	0.09	6.48E-108	Significant
32	2500-4500	April1SWE	33.85	0.13	3.28E-251	Significant
33	2500-4500	SwS	19.09	0.08	3.03E-81	Significant
34	2500-4500	SWEduration	3.64	0.01	2.80E-04	Significant
35	2500-4500	MaxSWE.dowy	-11.11	-0.04	1.14E-28	Significant
36	2500-4500	SDD	9.20	0.06	3.58E-20	Significant

These results are based on randomly generated 1000 points in each elevation band of our study domain.